Therapeutics, Targets, and Chemical Biology

Cancer Research

Transplanting Normal Vascular Proangiogenic Cells to Tumor-Bearing Mice Triggers Vascular Remodeling and Reduces Hypoxia in Tumors

Junpei Sasajima[1], Yusuke Mizukami[1], Yoshiaki Sugiyama[1], Kazumasa Nakamura[1], Toru Kawamoto[1], Kazuya Koizumi[1], Rie Fujii[1], Wataru Motomura[1], Kazuya Sato[1], Yasuaki Suzuki[1], Satoshi Tanno[1], Mikihiro Fujiya[1], Katsunori Sasaki[1], Norihiko Shimizu[2], Hidenori Karasaki[3], Toru Kono[3], Jun-ichi Kawabe[4], Masaaki Ii[5], Hiroki Yoshiara[6], Naohisa Kamiyama[6], Toshifumi Ashida[7], Nabeel Bardeesy[8], Daniel C. Chung[8], and Yutaka Kohgo[1]

Abstract

Blood vessels deliver oxygen and nutrients to tissues, and vascular networks are spatially organized to meet the metabolic needs for maintaining homeostasis. In contrast, the vasculature of tumors is immature and leaky, resulting in insufficient delivery of nutrients and oxygen. Vasculogenic processes occur normally in adult tissues to repair "injured" blood vessels, leading us to hypothesize that bone marrow mononuclear cells (BMMNC) may be able to restore appropriate vessel function in the tumor vasculature. Culturing BMMNCs in endothelial growth medium resulted in the early outgrowth of spindle-shaped attached cells expressing CD11b/Flt1/Tie2/c-Kit/CXCR4 with proangiogenic activity. Intravenous administration of these cultured vascular proangiogenic cells (VPC) into nude mice bearing pancreatic cancer xenografts and *Pdx1-Cre;LSL-Kras^{G12D};p53$^{lox/+}$* genetically engineered mice that develop pancreatic ductal adenocarcinoma significantly reduced areas of hypoxia without enhancing tumor growth. The resulting vasculature structurally mimicked normal vessels with intensive pericyte coverage. Increases in vascularized areas within VPC-injected xenografts were visualized with an ultrasound diagnostic system during injection of a microbubble-based contrast agent (Sonazoid), indicating a functional "normalization" of the tumor vasculature. In addition, gene expression profiles in the VPC-transplanted xenografts revealed a marked reduction in major factors involved in drug resistance and "stemness" of cancer cells. Together, our findings identify a novel alternate approach to regulate abnormal tumor vessels, offering the potential to improve the delivery and efficacy of anticancer drugs to hypoxic tumors. *Cancer Res; 70(15); 6283–92. ©2010 AACR.*

Introduction

Blood vessels deliver oxygen and nutrients to tissues, and vascular networks are spatially organized to meet the metabolic needs to maintain homeostasis (1). Regions of severe oxygen deprivation (hypoxia) arise in tumors due to rapid cell division and aberrant blood vessel formation (2). The vascular networks are usually disordered, chaotic, and highly leaky, resulting in an insufficient blood supply and, in general, contributing to tumor hypoxia (3). These structural and functional abnormalities of tumor vessels are a hallmark of solid tumors, one that contributes directly to the malignant properties of cancer (2, 4). Hypoxic tumors are usually resistant to conventional chemotherapy and radiotherapies, which typically target actively dividing cells (5), and accumulating evidence indicates that hypoxia has the potential to inhibit tumor cell differentiation and induce quiescence, allowing cancer cells to acquire a phenotype of "stemness" (2, 4). To "normalize" this aberrant tumor vasculature, therapies targeting vascular endothelial growth factor (VEGF) or its cognate receptor have shown clinical success in various human cancers (6–8). However, antiangiogenic therapy is not always effective, and intrinsic resistance to this novel therapy has been shown in some desmoplastic and hypovascular tumors, including pancreatic ductal adenocarcinoma (PDAC; ref. 9). In addition, antiangiogenic therapy may alter the natural history of tumors by inducing an invasive and metastatic phenotype (10).

Authors' Affiliations: [1]Division of Gastroenterology and Hematology/Oncology, Department of Medicine, [2]Department of Animal Facility, [3]Division of Gastroenterological and General Surgery, Department of Surgery, and [4]Department of Cardiovascular Regeneration and Innovation, Asahikawa Medical College, Asahikawa, Hokkaido, Japan; [5]Department of Pharmacology, Osaka Medical College, Osaka, Japan; [6]Toshiba Medical Systems Corp., Otawara, Tochigi, Japan; [7]Center for IBD, Sapporo Higashi Tokusyukai Hospital, Sapporo, Hokkaido, Japan; and [8]Massachusetts General Hospital and Harvard Medical School, Boston, Massachusetts

Note: Supplementary data for this article are available at Cancer Research Online (http://cancerres.aacrjournals.org/).

Corresponding Author: Yusuke Mizukami, Division of Gastroenterology and Hematology/Oncology, Department of Medicine, Asahikawa Medical College, 2-1 Midorigaoka-Higashi, Asahikawa, Hokkaido 078-8510, Japan. Phone: 81-1-666-82462; Fax: 81-1-666-82469; E-mail: mizu@asahikawa-med.ac.jp.

doi: 10.1158/0008-5472.CAN-10-0412

In view of the vasculogenic process that normally occurs in adult tissues under certain conditions to repair "injured" or newly formed blood vessels, bone marrow (BM)–derived cells have therapeutic potential to restore appropriate vessel function. Angiogenesis has been shown to play a central role in the recovery of the injured tissues including myocardial infarction. We and others have identified BM-derived proangiogenic cells that accumulate in active angiogenic foci and participate in neovascularization after ischemic insult, a concept consistent with postnatal vasculogenesis (11–13). These immature BM-derived cells, which include stem/progenitor cells, can enhance angiogenesis in ischemic heart in mice and protect injured tissues from fibrosis, an unfavorable form of tissue remodeling (11). Therefore, we were curious to determine whether bone marrow mononuclear cells (BMMNC) can also "repair" chaotic tumor vessels and tested this hypothesis using PDAC as a model for a hypoxic tumor. We also speculated that oxygen tension may be restored if the disordered vasculature in solid tumors could be manipulated, which potentially represents a compelling therapeutic intervention against hypoxic tumors.

In the current study, we propose an alternative approach to reorganize the abnormal tumor vasculature, which can potentially improve the delivery and efficacy of anticancer drugs against hypoxic tumors.

Materials and Methods

Cell culture

Three human pancreatic adenocarcinoma cell lines, KP-1N (from Health Science Research Resources Bank, Osaka, Japan), Panc-1, and BxPC-3 [both from the American Type Culture Collection (ATCC)], and four extrapancreatic cancer cell lines, MKN-28 (from Health Science Research Resources Bank), SW480, HepG2, and PC-9 (from ATCC), were used in this study.

The hypoxic workstation INVIVO$_2$ 400 (Ruskinn) was used to mimic hypoxic conditions in the tumor microenvironment. Cells were cultured at 5% O_2, 5% CO_2 for 1 month to adapt to hypoxic conditions, and cell viability was assessed by WST-8 assay in normoxic (20% O_2) and hypoxic (5% O_2) conditions (Quick Cell Proliferation Assay Kit, Biovision; ref. 14). Briefly, cancer cells were plated in 96-well plates (1×10^3–5×10^3 per well) and grown up to 72 hours, and the number of cells was quantified using a microtiter plate reader at 450 nm according to the manufacturer's instructions.

Animals, cell transplantation, and immunohistochemistry

Protocols for animal experiments were approved by the Asahikawa Medical College Institutional Animal Care and Use Committee. Cancer cells were injected s.c. into female CD-1 nude mice and the xenograft volume was calculated as (length × width^2) × 0.5. Tumors were grown to a minimum volume of 125 mm^3 before vascular proangiogenic cell (VPC) transplantation. Therapeutic studies were also performed using genetically engineered *Pdx1-Cre;LSL-Kras^{G12D};p53$^{lox/+}$* mice, which spontaneously develop PDAC with abundant desmoplasia (15), at 12 weeks of age when PDAC lesions were identified by an ultrasound diagnostic system (Aplio XG, Toshiba Medical Systems).

Murine BMMNCs were isolated by density gradient centrifugation using Histopaque-1083 (Sigma) and cultured in EBM2 with supplements (EGM2-MV BulletKit, Lonza) and 10% fetal bovine serum but without hydrocortisone in rat vitronectin (Sigma)-coated dishes for preparation of VPCs (13, 16). Attached cells were suspended at 4 days and reseeded to a new culture dish for VPC transplantation into tumor-bearing mice at day 7. More than 95% of attached cells were positive for acetylated low-density lipoprotein (Biomedical Technologies) uptake and BS1 lectin (Vector laboratories) binding, confirming endothelial and/or monocytic lineage (13, 17). The majority of the cells expressed CD11b as shown by flow cytometry, indicating that these cells were composed of heterogeneous populations including vascular leukocytes (18, 19). In addition to the expression of Tie2, a significant fraction of the attached BMMNCs expressed Flt1, CXCR4, and platelet-derived growth factor receptor β (PDGFR-β). Weak expression of the progenitor markers such as c-Kit and CD34 was also identified (antibody was purchased from Beckman Coulter and BD; Supplementary Fig. S1). Although genes expressed in endothelial cells such as *Flk-1* and *VE-cadherin* were upregulated in the BMMNCs during 7 days of culture as compared with freshly isolated CD11b$^+$ BMMNCs, there was a substantial induction of PDGFR-β mRNA.

The tumor-bearing mice were divided randomly into saline-infused or VPC-treated groups when PDAC tumors were established. The proangiogenic cells were prepared from BMMNCs isolated from syngeneic mice and the transplantation was performed through the retro-orbital cavity. Initially, 10^4, 10^5, and 10^6 VPCs were injected into nude mice bearing KP-1N xenografts (n = 10 for each group), and the growth of tumors was observed for up to 6 weeks. Because we observed effects of VPC transplantation histologically when 10^5 to 10^6 cells were injected, additional studies were then performed by transplanting larger numbers of VPCs. Tumor-bearing mice also received VPCs or a saline injection weekly for 2 to 3 weeks at 4- to 7-day intervals before sacrifice. To clarify whether transplanted VPCs were indeed localized to tumors, we injected green fluorescent protein (GFP)–labeled VPCs into mice (5×10^5 per mice) with PDAC xenografts in some of the experiments (13).

To assess hypoxic regions, pimonidazole hydrochloride (60 mg/kg; Hypoxyprobe-1, Millipore) was injected i.p. 1.5 hours before killing. We harvested xenograft tumors before the lesions reached 10 mm in diameter (the average volume was 200–300 mm^3) for histologic analysis. Tumor tissues were then fixed with zinc-fixative solution (IHC ZINC fixative, BD Pharmingen) for 24 hours at room temperature and embedded in paraffin for immunohistochemistry. For immunofluorescence staining in xenograft tissue, 4-μm sections were incubated with a CD31-specific antibody, MEC13.3 (1:50; BD Pharmingen), overnight at 4°C. Blood vessels were counted in 5 to 10 random viable fields (20× objective), and the vessel area/density was quantified using ImageJ software (version 1.38). For other immunohistochemical studies, the following antibodies were used: anti-MIB-1 (DAKO; 1:100), anti-NG2 (Chemicon; 1:200), anti–cleaved caspase-3 (5A1E, Cell Signaling; 1:200), and anti-CA9 (Novus; 1:100). Nuclei were

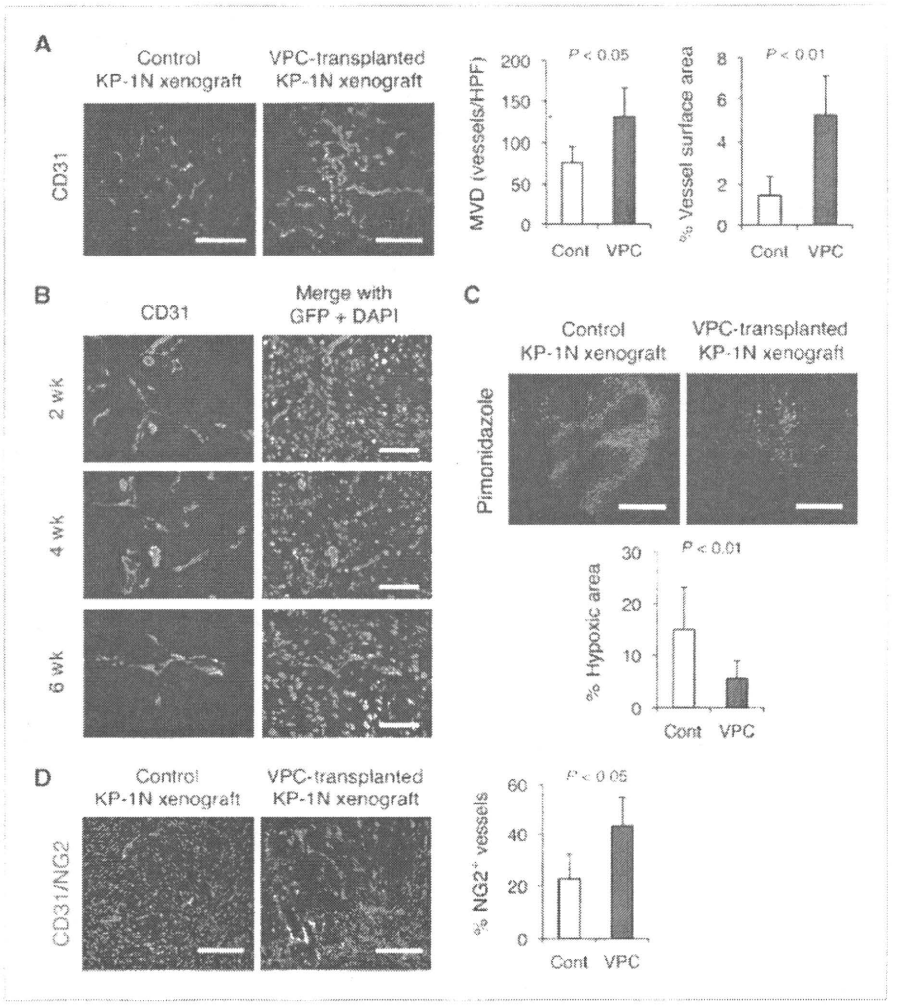

Figure 1. Intravenous transplantation of *ex vivo* cultured CD11b$^+$ VPCs induces vascular remodeling and reduces tumor hypoxia in KP-1N xenografts. A, VPC transplantation (5×10^5 cells) was performed in CD-1 nude mice bearing KP-1N xenografts, and mice were sacrificed 2 wk after transplantation. The tumor sections were stained with CD31. Columns, mean microvessel density (MVD) and vessel surface area; bars, SEM. HPF, high-power field. B, to trace transplanted cells, VPCs prepared using GFP-labeled BMMNCs were i.v. injected into mice with KP-1N xenografts. Mice were sacrificed 2 to 6 wk after and the tumor sections were stained with anti-CD31 and anti-GFP. Bar, 100 μm. C, to assess hypoxic regions, frozen sections were stained with anti–Hypoxyprobe-1 antibody. Positive staining area was shown as hypoxic area in xenografts. D, double immunofluorescent staining with NG2 and CD31. The number of CD31$^+$ microvessels covered with NG2 positive pericytes is shown. Bar, 500 μm.

counterstained with 50 ng/mL 4′,6-diamidino-2-phenylindole (Sigma) and images were examined with a fluorescent microscope (BX-51/DP-71, Olympus).

To visualize the extracellular matrix in xenograft tumors, tissue staining was performed using Masson's trichrome kit (Sigma-Aldrich) according to the manufacturer's protocol.

In vivo vascular imaging by contrast-enhanced ultrasound system

To visualize perfusion within tumors, an ultrasound contrast agent, Sonazoid (Daiichi-Sankyo Co. Ltd.), was administered to tumor-bearing mice (0.25 μL/kg). The vascularized area within tumors was imaged by an ultrasound diagnostic system (AplioXG, Toshiba Medical Systems Corp.) with a 12-MHz linear probe (PLT-1204AT). The phase modulation harmonic imaging mode (transmitted/received at 5.0/10.0 MHz) was used for the nonlinear signal extraction, and the mechanical index was set to around 0.20. The images for 30 seconds after injection were recorded into the U.S. system and transferred to consumer PC after the experiments.

The arrival time parametric images were reconstructed by using the dedicated prototype software programmed by C++ (20). The software reads the Audio Video Interleaving (AVI) image obtained by the U.S. system, calculates the enhanced intensity on the image frame by frame, and paints the colors, which correspond to the time to arrival of the enhancement. Because each color has the numerical value of the arrival, the arrival time of each part will be indicated by the still image of the resulting parametric imaging.

Quantitative real-time PCR assay

Total RNA was extracted using the RNeasy Protect Mini kit (QIAGEN) according to the manufacturer's instructions. TaqMan Gene Expression Assay primer and probe sets (Applied Biosystems) were used for quantitative real-time PCR analysis. The primer sequences are summarized in Supplementary Table S1. Transcript levels were normalized to 18S rRNA. Results are expressed as normalized expression values ($2^{-\Delta CT}$) or normalized expression relative to control cells or tissues without cell transplantation (= $2^{-\Delta\Delta CT}$), unless otherwise stated.

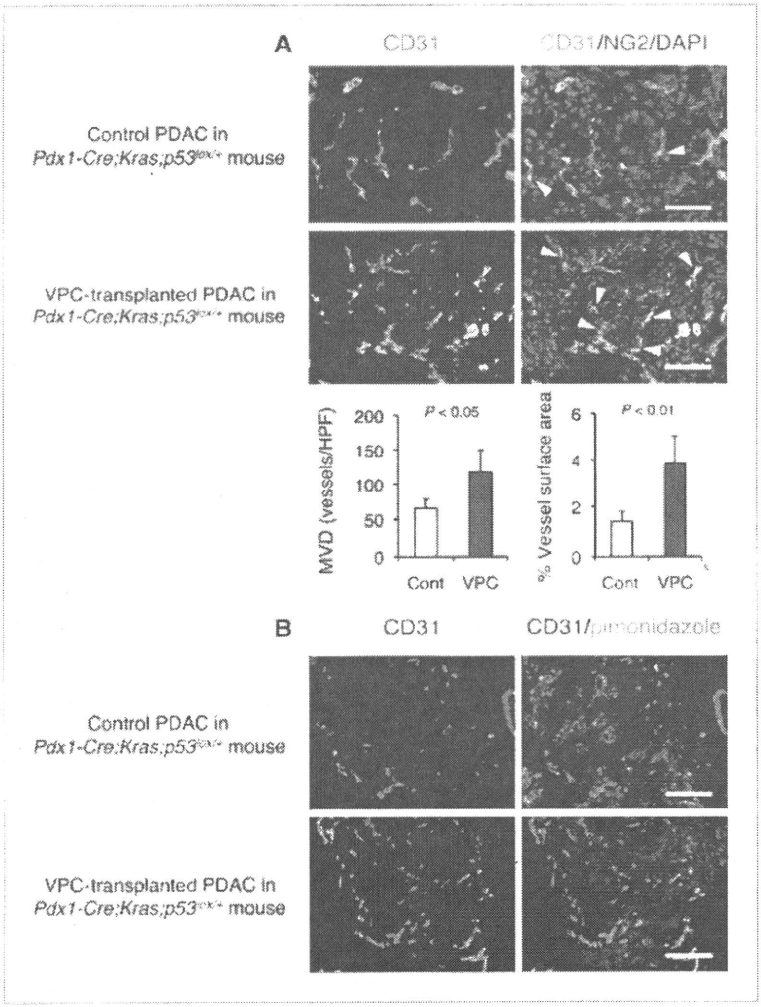

Figure 2. Transplantation of VPCs promotes maturation of the tumor vasculature, resulting in reduced hypoxic area in spontaneously developed PDAC. Sequential VPC transplantation (5×10^5; twice) was performed in *Pdx1-Cre;LSL-Kras^{G12D};p53$^{lox/+}$* mice (12 wk old), and mice were sacrificed 2 wk after transplantation. A, double immunofluorescent staining with NG2 and CD31 in zinc-fixed sections. Arrowheads, NG2$^+$ pericyte–covered microvessels. B, double immunofluorescent staining with anti–Hypoxyprobe-1 and anti-CD31 in frozen sections. Bar, 100 μm.

Statistical analysis

All results are expressed as mean ± SD unless otherwise noted. The statistical significance of differences was determined using two-tailed Student's *t* test.

Results and Discussion

Transplantation of cultured VPCs into tumor-bearing mice induces vascular remodeling and reduces tumor hypoxia

To determine whether cultured CD11b$^+$ VPCs possess a capacity to repair tumor vessels, we performed a series of investigations using spindle-shaped attached BM mononuclear cells cultured in EGM2 medium as crude proangiogenic cells (Supplementary Fig. S1). PDAC was selected as a model for a hypoxic tumor to test our hypothesis that certain malignant phenotypes associated with hypoxia may be abolished if abnormalities of the tumor vasculature could be appropriately manipulated. Intravenous administration of 5×10^5 VPCs into nude mice bearing KP-1N human pancreatic cancer xenografts significantly increased tumor microvessel density (Fig. 1A). The transplanted cells localized to the perivascular area, closely associating with the tumor vasculature rather than directly differentiating into vascular endothelial cells (Fig. 1B). In addition, the number of GFP$^+$ transplanted cells was significantly attenuated at 6 weeks after transplantation, suggesting that the *ex vivo* cultured VPCs may not constitute blood vessels for long term. In contrast to the narrowed and fragmented vasculature in control xenografts, the vessel surface area in VPC-transplanted tumors was dramatically increased (1.5 ± 0.9% versus 5.3 ± 1.8%; $P < 0.01$). The enlarged tumor vasculature seemed to be functional because it was accompanied by reduced areas of tumor hypoxia as represented by pimonidazole-positive areas within the tumor (Fig. 1C). In addition, increases in vascularized (perfused) areas within VPC-injected xenografts were observed by arrival time parametric imaging reconstructed from images by an ultrasound diagnostic system with a 12-MHz linear probe during injection of a contrast agent (Sonazoid) when serial i.v. injections of 10^5 VPCs three times at 4-day intervals were

performed (Supplementary Fig. S2; Supplementary Materials 1 and 2), indicating a functional "reorganization/remodeling" of the abnormal tumor vasculature.

We next confirmed whether the tumor vessels in the VPC-transplanted tumor were structurally mature. Because pericytes play an essential role in the integrity of structural vessels, immunohistochemical staining for NG2 and CD31 was then performed (Fig. 1D). Increased numbers of $CD31^+$ microvessels were covered with $NG2^+$ pericytes, indicating that the resulting tumor vasculature structurally mimicked normal vessels with a high pericyte coverage ratio.

Similar observations were shown in genetically engineered *Pdx1-Cre;LSL-Kras^{G12D};p53$^{lox/+}$* mice, which spontaneously develop desmoplastic PDAC (15), and undifferentiated tissues with abundant desmoplasia were selected for histologic analysis. Poor tissue perfusion was also successfully corrected by VPC transplantation in this mouse model (Fig. 2). Therefore, the vascular regeneration/remodeling through the cell-mediated approach is not limited to artificial xenograft tumors but is also capable of manipulating abnormal blood perfusion in spontaneously developing desmoplastic PDAC tumors in mice.

Transplantation of cultured $CD11b^+$ VPCs does not enhance tumor growth but instead temporarily delays the outgrowth

Because tumor outgrowth is generally dependent on angiogenesis, we initially speculated that enhanced blood perfusion may promote tumor growth and metastasis. However, to our surprise, the growth of PDAC xenografts was significantly inhibited when more than 10^5 VPCs were transplanted (Fig. 3A). When tumor growth was observed for 6 weeks post-transplantation, the growth of xenograft tumors was temporarily slowed by VPC transplantation although they started to regrow within 3 weeks (Fig. 3B). To determine whether this reduction of tumor growth can also be observed in other cell types, additional xenograft experiments were then performed using various human cancer cell lines (Supplementary Table S2). Serial i.v. injections of 5×10^5 VPCs were performed subsequent to xenograft establishment at 7-day intervals. A significant reduction in tumor growth was observed in other human pancreatic cancer cells, Panc-1 and BxPC-3. Additionally, growth inhibition of xenograft tumors was also shown in MKN-24 (a human gastric cancer cell line) and PC-9 (a human lung cancer cell line). Of note, enhancement of tumor growth was not induced by VPC transplantation in cells tested and metastatic outgrowth was not observed even in SW480 and hypervascular HepG2 xenografts.

Oxygen and nutrients are required for any tissue including tumors, but cancer cells can survive even in severe hypoxia (21). It is well known that most cancer cells rely on aerobic glycolysis, rather than mitochondrial oxidative phosphorylation, to generate energy needed for cellular processes (22). However, it should be noted that clinical trials have shown that reducing tissue hypoxia either through blood transfusion or erythropoietin could be associated with an improved response to radiotherapy and may improve the survival of cancer patients (23). In addition, a recent study showed that angiopoietin-1–mediated maturation of blood vessels can inhibit tumor growth through a suppression of permeability in tumors with pericyte-rich blood vessels (24). We therefore sought to address the question of whether the tumor microenvironment with abundant oxygen delivered by reorganized blood vessels is favorable for tumor cells or not.

Histopathologic analysis revealed that transplantation of cultured $CD11b^+$ VPCs did not significantly increase areas of necrosis (Fig. 4A). Masson's trichrome staining showed that xenograft tumors in the VPC-transplanted mice were depleted of desmoplastic stroma, resulting in densely packed ductal adenocarcinoma cells (Supplementary Fig. S3), and the number of cells per area was increased by VPC transplantation, suggesting that VPCs increase the density of cells. This could thereby facilitate the blood perfusion in PDAC indirectly. Similar observations have been made with VPC transplantation into mouse models of acute coronary ischemia (25, 26); that is, tissue remodeling composed of extensive fibrosis in infarct heart and cirrhotic liver could be attenuated by transplantation of BMMNCs manipulated by a similar *ex vivo* differentiation protocol (27).

To directly address the effect of oxygen during reperfusion (reoxygenation) in hypoxic tumors, we performed an *in vitro*

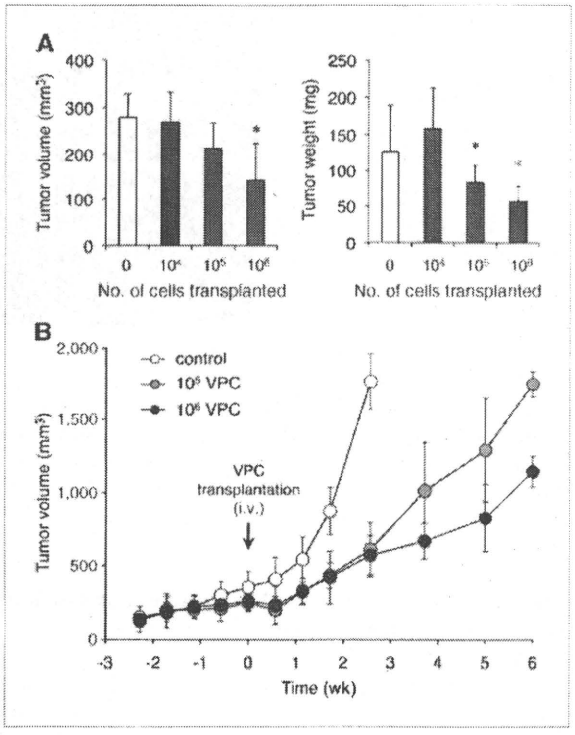

Figure 3. VPC transplantation does not stimulate tumor outgrowth in KP-1N xenografts. VPCs (10^4, 10^5, and 10^6) were injected into nude mice bearing KP-1N xenografts (n = 10 for each group). A, tumor volume (left) and tumor weight (right) of KP-1N xenografts with or without VPC transplantation. *, $P < 0.05$, versus control mice (PBS injected). B, growth of KP-1N xenografts with or without VPC transplantation was observed for up to 6 wk (PBS or 10^5 or 10^6 VPCs injected; n = 6 for each). Mice were humanely killed following development of a tumor larger than 2,000 mm^3 or a tumor harboring an ulcer.

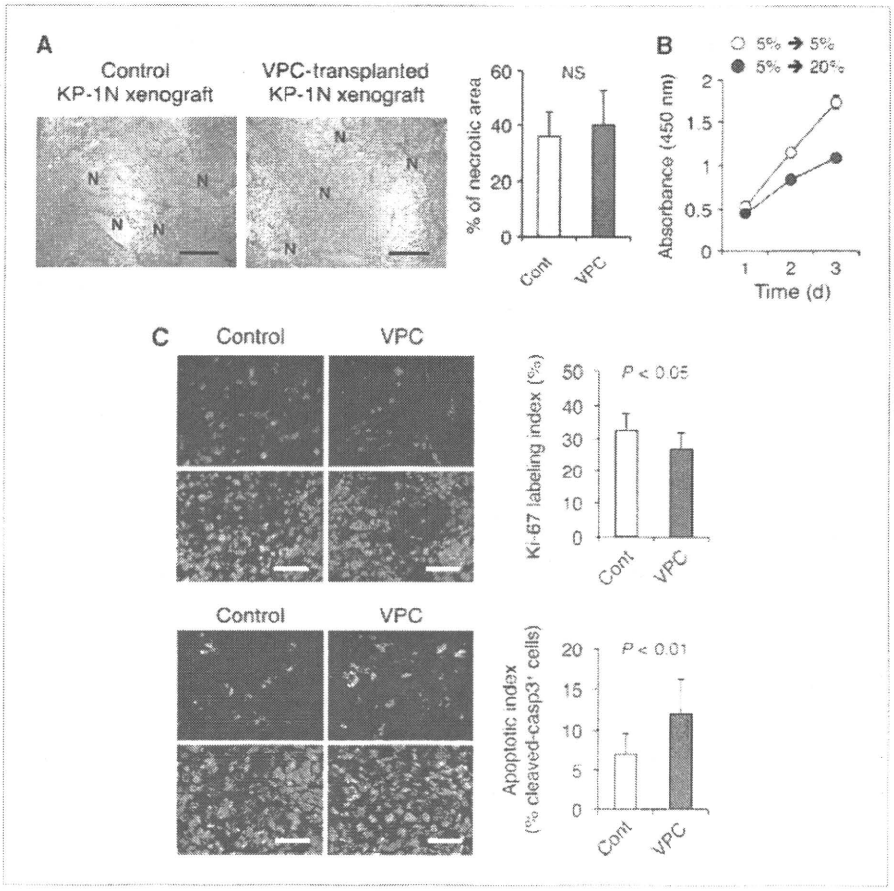

Figure 4. Transplantation of *ex vivo* cultured VPCs impairs the growth of KP-1N xenografts. A, KP-1N xenografts were treated with or without i.v. administration of cultured VPCs (5×10^5; twice) and mice were sacrificed 2 wk after the procedure. H&E stainings for xenograft sections are shown and percent necrotic area (N) was measured. Bar, 200 μm. B, KP-1N cells adapted to chronic hypoxia (5% O_2 in hypoxia workstation INVIVO$_2$ 400) were cultured either in normoxic (20% O_2) or in hypoxic conditions (5% O_2) for 3 d. Cell growth was quantified by WST-8 assay. C, xenograft tissues were stained with anti–Ki-67 (top) and anti–cleaved caspase-3 (bottom). Quantification of proliferating/apoptotic is shown as percent positive cells in 5 viable fields from 10 sections. Bar, 100 μm. Columns, mean proliferation/apoptotic index; bars, SEM.

assay using PDAC cells adapted to long-term hypoxic conditions under low oxygen tension (5% O_2) by using a hypoxia workstation. Although hypoxia generally downregulates cell proliferation (28), the KP-1N human PDAC line adapted to 5% O_2 (chronic hypoxia) can grow equally with a comparable doubling time as cells cultured in normoxic conditions (20% O_2; doubling time in chronic hypoxia and normoxic conditions was 21.0 ± 2.8 and 22.8 ± 3.1 hours, respectively). However, the proliferation of the hypoxia-conditioned KP-1N cells was significantly attenuated when the cells were placed again under normoxic conditions (doubling time, 31.7 ± 4.8 hours; $P < 0.01$; Fig. 4B). A similar observation was also shown in primary mouse PDAC cells from *Pdx1-Cre;LSL-Kras^{G12D};p53$^{lox/+}$* mice (doubling time was 13.6 ± 2.5 hours in chronic hypoxia and 16.7 ± 2.9 hours in reoxygenated cells; $P < 0.05$). These results may account for the attenuated tumor growth when the tumor vasculature was reorganized/remodeled by the *ex vivo* cultured CD11b$^+$ VPC transplantation that liberated PDAC cells from hypoxic conditions.

We therefore examined the effect of serial VPC transplantation (5×10^5 cells; 7-day intervals) on the proliferation kinetics of xenograft tumors *in vivo*. There was a modest but statistically significant difference in the Ki-67 labeling index (Fig. 4C), consistent with the growth retardation by VPC transplantation. Because staining the xenograft tissues for Ki-67 showed a reduced proliferation of cancer cells by only 17.6%, additional immunostaining using anti–cleaved caspase-3 was then performed. The apoptotic fraction was markedly increased by 1.72-fold in xenograft tumors when cultured VPCs were serially transplanted (Fig. 4C). These results indicate that enhanced blood perfusion may impair the ability of tumor cells to rapidly grow. The remodeling of abnormal tumor vasculature induces reperfusion of hypoxic tissue and reduced areas of significant hypoxia (Figs. 1 and 2). This potentially leads to an increase in free radical concentration, resulting in growth suppression through an induction of stress-response genes (21, 29).

Transplantation of cultured CD11b$^+$ VPCs attenuates angiogenic cytokine production from cancer cells during reperfusion in PDAC xenografts

VPC transplantation induced repair of the abnormal tumor vasculature and reduced tumor desmoplasia, which could further facilitate blood perfusion. This histologic remodeling may also attenuate oxygen consumption by the microenvironment. We therefore speculated that transplantation of cultured CD11b$^+$ VPCs may alter the imbalance between proangiogenic and antiangiogenic cytokines released from

tumor cells. In general, cancer cells express excess amounts of various proangiogenic factors, which primarily regulate the abnormal tumor vasculature. To test this possibility, we quantified the mRNA levels of proangiogenic factors from cancer cells in xenografts by using human-specific probes. Consistent with the marked reduction in tumor hypoxia, the VEGF mRNA levels were significantly attenuated (Fig. 5). Interleukin-8, another proangiogenic cytokine that can be induced by hypoxia in cells with oncogenic Kras (30), was also strongly downregulated. Pigment epithelium–derived factor (PEDF) is a potent angiogenic inhibitor in the pancreas, expressed by both epithelial and stromal compartments and regulated by hypoxia. PEDF expression has been shown to be downregulated during pancreatic tumorigenesis, at least in part playing a role in neovascularization and metastatic outgrowth in PDAC (31, 32). Curiously, VPC transplantation restored PEDF expression in cancer cells, which may account for not only the reduction in aberrant tumor angiogenesis but also the inhibition of proliferation of tumor cells.

Because Masson's trichrome staining showed that the transplantation of cultured VPCs significantly reduced the amount of desmoplastic stroma, we speculated that genes involved in fibrosis may also be altered. There was no significant difference in the mRNA levels of cancer cell–derived transforming growth factor-β and osteopontin (27, 33), known fibrosis mediators, and the precise mechanisms by which VPC transplantation reduced PDAC desmoplasia need to be further elucidated. However, The Ihh morphogen, but not Shh, which plays a role in pancreatic fibrosis through an activation of pancreatic stellate cells (34), was downregulated by regeneration of the tumor vasculature in PDAC xenografts. There was upregulation of desmoplasia-related α2 (type I) procollagen (*COL1A2*) and secreted protein acidic and rich in cysteine (*SPARC*) genes in tumor cells when VPCs were transplanted; however, the levels were modest when compared with their stromal expression, where VPC transplantation had no influence. Taken together, these data indicate that transplanted VPCs localized to hypoxic areas either in tumors or in infarcted (ischemic) heart may have the capacity to terminate abnormal tissue remodeling including aberrant angiogenesis.

Cancer cells released from hypoxia represent a phenotype with less resistance to chemotherapy and reduced stemness phenotype

Expression of carbonic anhydrase 9 (CA9), one of the hypoxia-inducible factor (HIF) target genes, has been proposed as a marker of prolonged hypoxia (35). CA9 plays a role in maintaining an alkaline intracellular pH and an acidic extracellular pH (36, 37) and in anchorage-independent tumor cell growth, facilitating invasion of cancer cells into the extracellular matrix by modulating the functions of E-cadherin (38). We therefore examined CA9 expression by immunohistochemistry in VPC-transplanted tumors (Fig. 6A). In line with a significant reduction in pimonidazole-positive areas in xenografts receiving VPC injections, the resulting vascular remodeling also attenuated the number of CA9-positive cells dramatically. The reduction was more prominent in viable areas as compared with perinecrotic areas.

Hypoxia and HIFs have been shown to activate signaling pathways that control stem cell self-renewal and multipotency (39). In addition to hematologic malignancies, solid tumors can also develop from a small number of self-renewing transformed cells, the so-called tumor-initiating cells (40).

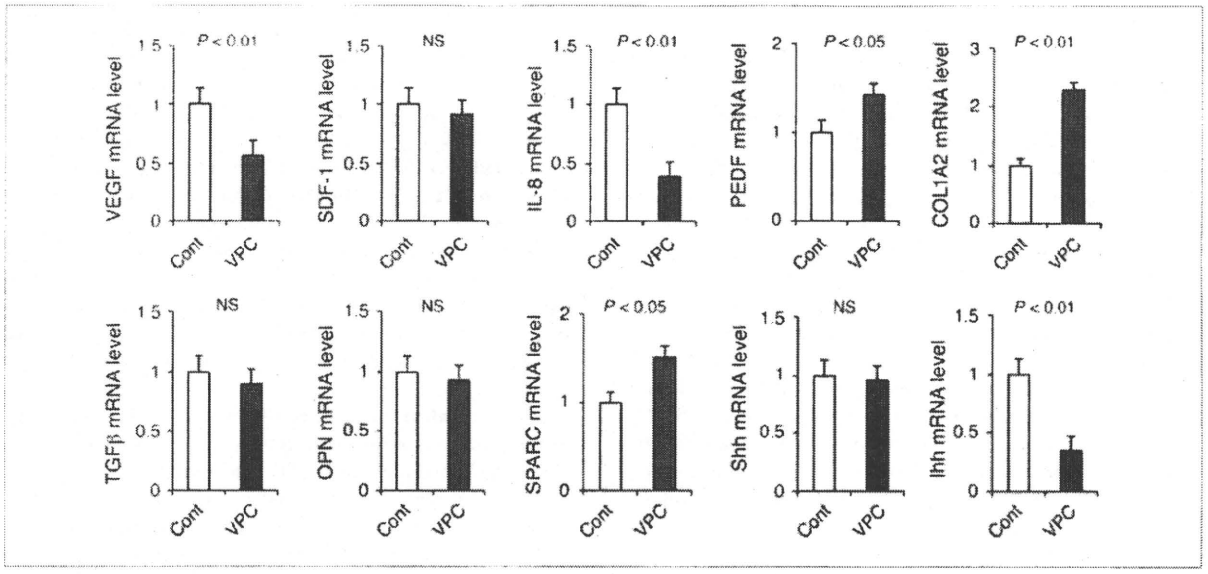

Figure 5. Transplantation of VPCs terminates aberrant neovascularization by attenuating angiogenic cytokine production from cancer cells. RNA was extracted from xenograft tissues treated with or without VPC transplantation, and mRNA levels of proangiogenic and antiangiogenic factors in cancer cells were analyzed by TaqMan quantitative PCR. Alterations in gene expression associated with desmoplasia are also shown. SDF-1, stromal cell–derived factor 1; IL-8, interleukin-8; TGFβ, transforming growth factor β; OPN, osteopontin.

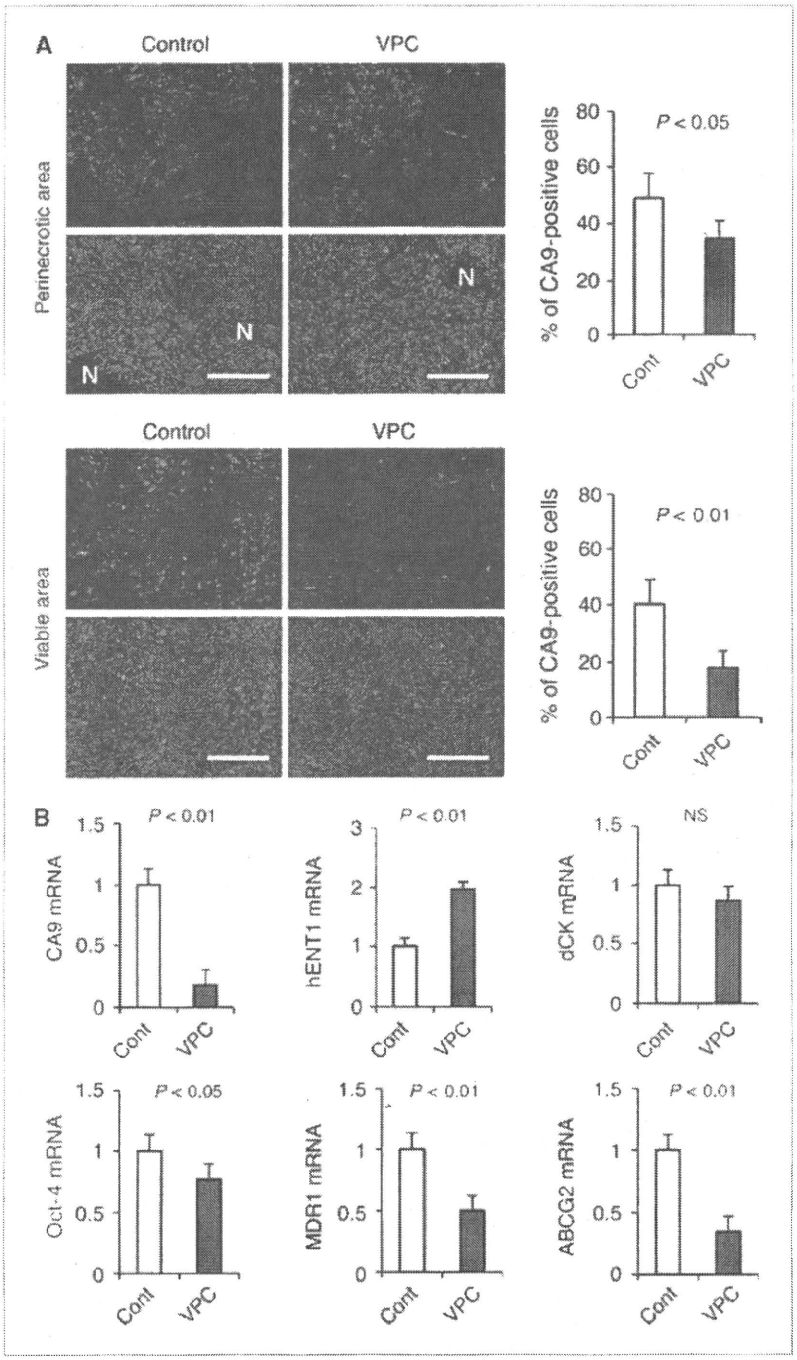

Figure 6. Reduction in tumor hypoxia reduces CA9 expression and gene expression–related drug resistance and stemness. KP-1N xenografts were treated with or without i.v. administration of cultured VPCs (10^5; three times) and mice were sacrificed 2 wk after the procedure. A, xenograft tissues were stained with anti-CA9 in either perinecrotic (top) or viable area (bottom). Quantification of CA9-positive cells is shown in 5 viable fields from 6 sections. Bar, 500 μm. N, necrotic area. B, RNA was extracted from xenograft tissues, and mRNA levels of CA9, Oct-4, hENT1, dCK, MDR-1 (ABCB1), and ABCG2 in cancer cells in xenografts were analyzed by TaqMan quantitative PCR.

Accumulating evidence has indicated that these rare types of cancer cells with stemness properties can localize in a "hypoxic niche," giving rise to resistance to chemotherapy and radiotherapy (4). This implies that regional hypoxia plays a fundamental role in both regulating the stemness properties of cancer cells and diminishing therapeutic response and that both of the hypoxia-induced phenotypes could be reversible. We therefore sought to determine whether vascular remodeling induced by VPC transplantation may alter such stemness and resistant phenotypes of hypoxic PDAC cells. Xenograft tumors were used to specifically analyze gene expression in cancer cells rather than stromal cells, using human-specific probes for TaqMan quantitative PCR assays (Fig. 6B). There was a significant reduction in CA9 mRNA levels in VPC-transplanted xenografts, consistent with a massive reduction in CA9 immunostaining (Fig. 6A).

Octamer-binding transcription factor 4 (*Oct-4*), one of the stemness genes that can induce pluripotency in differentiated cells (41), was downregulated by 22.9%. Because HIF-2α can directly regulate *Oct-4*, it is therefore possible that hypoxia mediates its effects on stem cell function by altering the stemness genes (42). Considering that Oct-4 is involved in tumor progression and motility (43), downregulation of Oct-4 would be beneficial to control the malignant phenotype caused by hypoxia. Additionally, the expression levels of *MDR1* (*ABCB1*) and *ABCG2*, genes that play a major role in "resistance" to chemotherapy, were also dramatically downregulated by VPC transplantation (Fig. 6B).

Gemcitabine is the standard chemotherapeutic reagent for locally advanced or metastatic PDAC (44), and a recent study performed on cultured PDAC cells indicated that human equilibrative nucleoside transporter-1 (hENT1) is the major transporter for gemcitabine, and increased hENT1 abundance facilitates efficient cellular entry of the drug and confers its increased cytotoxicity (14, 45). We found that there was a 2-fold induction of hNET1 mRNA in tumor cells when xenograft-bearing mice were treated with cultured CD11b$^+$ VPCs, consistent with the observation that hENT1 could be downregulated by hypoxia (46). Therefore, although we did not observe any differences in dCK mRNA, another important intracellular modulator of gemcitabine, PDACs with normalized blood vessels by VPC transplantation may be more sensitive to gemcitabine as compared with hypoxic tumors. Taken together, these data indicate that remodeling of an unstable tumor vasculature leads to a significant reduction in expression of genes associated with the stemness of cancer cells as well as an increase in sensitivity to conventional chemotherapy. We are currently testing this hypothesis by studying a combination of chemotherapeutic agents such as gemcitabine and VPC transplantation.

Conclusion

BM cells are thought to play a role in tumor development (47), and various types of BM-derived hematopoietic cells have been observed to closely associate with the tumor neovasculature (18, 48). Indeed, a small number of BM-derived progenitor cells were shown to incorporate into the lumen of a growing vasculature where they differentiate into endothelial cells in a mouse metastasis model (49). The BM-derived cells generally have been thought to augment the malignant phenotype of tumor; however, our data support the notion that certain immature myeloid cells from the BM may have the capacity to repair an abnormal microenvironment if they are appropriately differentiated *ex vivo*. In support of our results, others have also shown increases in blood flow within tumor xenografts when embryonic stem cell–derived VPCs were transplanted, and no enhancement of tumor growth was observed (50). In the current study, we observed that a considerable number of transplanted CD11b$^+$VPCs localized to the perivascular area, and therefore they did not seem to induce angiogenesis (vasculogenesis) by directly differentiating into vascular endothelial cells. Those transplanted cells have been shown to promote neovascularization indirectly through paracrine stimulation/stabilization of neovessels (11). We found that, in addition to VEGF and angiopoietin-1, the cultured VPCs also express significant levels of antiangiogenic factors (51), suggesting their potential role in terminating aberrant neovascularization. Further studies are required to address the precise mechanisms by which these *ex vivo* cultured BMMNCs influence the chaotic blood vessels and tumor microenvironment. Our study also implies that the potential risk of enhancing tumor growth may not be an issue during cell therapy using progenitors, at least if cultured (manipulated) cells are used.

Collectively, we have identified an alternative approach to regulate the abnormal tumor vasculature. Tumor vessels remodeled by *ex vivo* cultured CD11b$^+$ VPCs exhibited maturation of the "abnormal" vasculature, resulting in a significant reduction in tumor hypoxia. The cancer cells seemed to have a distinct phenotype in the reperfused/reoxygenated microenvironment with decreased stemness-related gene expressions. This approach may not only attenuate innate resistance to chemotherapy/radiotherapy but also potentially improve the delivery of anticancer drugs to hypoxic tumors.

Disclosure of Potential Conflicts of Interest

No potential conflicts of interest were disclosed.

Acknowledgments

We thank Shizuo Kato for his assistance in tissue section preparation, Yasuhiko Nagasaka (Beckman Coulter) for technical assistance in flow cytometry analysis, and Kotoe Shibusa for BMMNC collection and cell sorting. We also thank to Azusa Tsukada (Toshiba Medical Systems) for assistance in obtaining contrast-enhanced ultrasound images and Dr. Hideki Kato (Hamamatsu University School of Medicine) for genetic testing of mice and helpful discussions.

Grant Support

New Energy and Industrial Technology Development Organization of Japan grant 07A05010a (Y. Mizukami).

The costs of publication of this article were defrayed in part by the payment of page charges. This article must therefore be hereby marked *advertisement* in accordance with 18 U.S.C. Section 1734 solely to indicate this fact.

Received 02/05/2010; revised 04/27/2010; accepted 05/24/2010; published OnlineFirst 07/14/2010.

References

1. Pugh CW, Ratcliffe PJ. Regulation of angiogenesis by hypoxia: role of the HIF system. Nat Med 2003;9:677–84.
2. Keith B, Simon MC. Hypoxia-inducible factors, stem cells, and cancer. Cell 2007;129:465–72.
3. Carmeliet P, Jain RK. Angiogenesis in cancer and other diseases. Nature 2000;407:249–57.
4. Das B, Tsuchida R, Malkin D, Koren G, Baruchel S, Yeger H. Hypoxia enhances tumor stemness by increasing the invasive and tumorigenic side population fraction. Stem Cells 2008;26:1818–30.
5. Teicher BA. Hypoxia and drug resistance. Cancer Metastasis Rev 1994;13:139–68.
6. Hurwitz H, Fehrenbacher L, Novotny W, et al. Bevacizumab plus

irinotecan, fluorouracil, and leucovorin for metastatic colorectal cancer. N Engl J Med 2004;350:2335–42.
7. Sandler A, Gray R, Perry MC, et al. Paclitaxel-carboplatin alone or with bevacizumab for non-small-cell lung cancer. N Engl J Med 2006;355:2542–50.
8. Escudier B, Eisen T, Stadler WM, et al. Sorafenib in advanced clear-cell renal-cell carcinoma. N Engl J Med 2007;356:125–34.
9. Kindler HL, Friberg G, Singh DA, et al. Phase II trial of bevacizumab plus gemcitabine in patients with advanced pancreatic cancer. J Clin Oncol 2005;23:8033–40.
10. Paez-Ribes M, Allen E, Hudock J, et al. Antiangiogenic therapy elicits malignant progression of tumors to increased local invasion and distant metastasis. Cancer Cell 2009;15:220–31.
11. Ii M, Nishimura H, Iwakura A, et al. Endothelial progenitor cells are rapidly recruited to myocardium and mediate protective effect of ischemic preconditioning via "imported" nitric oxide synthase activity. Circulation 2005;111:1114–20.
12. Yamazaki M, Nakamura K, Mizukami Y, et al. Sonic hedgehog derived from human pancreatic cancer cells augments angiogenic function of endothelial progenitor cells. Cancer Sci 2008;99:1131–8.
13. Nakamura K, Sasajima J, Mizukami Y, et al. Hedgehog promotes neovascularization in pancreatic cancers by regulating Ang-1 and IGF-1 expression in bone-marrow derived pro-angiogenic cells. PLoS One 2010;5:e8824.
14. Nakano Y, Tanno S, Koizumi K, et al. Gemcitabine chemoresistance and molecular markers associated with gemcitabine transport and metabolism in human pancreatic cancer cells. Br J Cancer 2007;96:457–63.
15. Bardeesy N, Aguirre AJ, Chu GC, et al. Both p16(Ink4a) and the p19 (Arf)-p53 pathway constrain progression of pancreatic adenocarcinoma in the mouse. Proc Natl Acad Sci U S A 2006;103:5947–52.
16. Ii M, Takenaka H, Asai J, et al. Endothelial progenitor thrombospondin-1 mediates diabetes-induced delay in reendothelialization following arterial injury. Circ Res 2006;98:697–704.
17. Assmus B, Schachinger V, Teupe C, et al. Transplantation of Progenitor Cells and Regeneration Enhancement in Acute Myocardial Infarction (TOPCARE-AMI). Circulation 2002;106:3009–17.
18. Conejo-Garcia JR, Buckanovich RJ, Benencia F, et al. Vascular leukocytes contribute to tumor vascularization. Blood 2005;105:679–81.
19. Kim SJ, Kim JS, Papadopoulos J, et al. Circulating monocytes expressing CD31: implications for acute and chronic angiogenesis. Am J Pathol 2009;174:1972–80.
20. Sugimoto K, Moriyasu F, Kamiyama N, Metoki R, Iijima H. Parametric imaging of contrast ultrasound for the evaluation of neovascularization in liver tumors. Hepatol Res 2007;37:464–72.
21. Harris AL. Hypoxia-a key regulatory factor in tumour growth. Nat Rev Cancer 2002;2:38–47.
22. Chen Y, Cairns R, Papandreou I, Koong A, Denko NC. Oxygen consumption can regulate the growth of tumors, a new perspective on the Warburg effect. PLoS One 2009;4:e7033.
23. Rades D, Tribius S, Yekebas EF, et al. Epoetin α improves survival after chemoradiation for stage III esophageal cancer: final results of a prospective observational study. Int J Radiat Oncol Biol Phys 2006; 65:459–65.
24. Satoh N, Yamada Y, Kinugasa Y, Takakura N. Angiopoietin-1 alters tumor growth by stabilizing blood vessels or by promoting angiogenesis. Cancer Sci 2008;99:2373–9.
25. Kawamoto A, Tkebuchava T, Yamaguchi J, et al. Intramyocardial transplantation of autologous endothelial progenitor cells for therapeutic neovascularization of myocardial ischemia. Circulation 2003; 107:461–8.
26. Cho HJ, Lee N, Lee JY, et al. Role of host tissues for sustained humoral effects after endothelial progenitor cell transplantation into the ischemic heart. J Exp Med 2007;204:3257–69.
27. Nakamura T, Torimura T, Sakamoto M, et al. Significance and therapeutic potential of endothelial progenitor cell transplantation in a cirrhotic liver rat model. Gastroenterology 2007;133:91–107, e1.
28. Carmeliet P, Dor Y, Herbert JM, et al. Role of HIF-1α in hypoxia-mediated apoptosis, cell proliferation and tumour angiogenesis. Nature 1998;394:485–90.
29. Yu G, Tseng GC, Yu YP, et al. CSR1 suppresses tumor growth and metastasis of prostate cancer. Am J Pathol 2006;168:597–607.
30. Mizukami Y, Jo WS, Duerr EM, et al. Induction of interleukin-8 preserves the angiogenic response in HIF-1α-deficient colon cancer cells. Nat Med 2005;11:992–7.
31. Doll JA, Stellmach VM, Bouck NP, et al. Pigment epithelium-derived factor regulates the vasculature and mass of the prostate and pancreas. Nat Med 2003;9:774–80.
32. Uehara H, Miyamoto M, Kato K, et al. Expression of pigment epithelium-derived factor decreases liver metastasis and correlates with favorable prognosis for patients with ductal pancreatic adenocarcinoma. Cancer Res 2004;64:3533–7.
33. Vetrone SA, Montecino-Rodriguez E, Kudryashova E, et al. Osteopontin promotes fibrosis in dystrophic mouse muscle by modulating immune cell subsets and intramuscular TGF-β. J Clin Invest 2009; 119:1583–94.
34. Shinozaki S, Ohnishi H, Hama K, et al. Indian hedgehog promotes the migration of rat activated pancreatic stellate cells by increasing membrane type-1 matrix metalloproteinase on the plasma membrane. J Cell Physiol 2008;216:38–46.
35. Olive PL, Aquino-Parsons C, MacPhail SH, et al. Carbonic anhydrase 9 as an endogenous marker for hypoxic cells in cervical cancer. Cancer Res 2001;61:8924–9.
36. Semenza GL. Regulation of cancer cell metabolism by hypoxia-inducible factor 1. Semin Cancer Biol 2009;19:12–6.
37. Swietach P, Vaughan-Jones RD, Harris AL. Regulation of tumor pH and the role of carbonic anhydrase 9. Cancer Metastasis Rev 2007; 26:299–310.
38. Svastova E, Zilka N, Zat'ovicova M, et al. Carbonic anhydrase IX reduces E-cadherin-mediated adhesion of MDCK cells via interaction with β-catenin. Exp Cell Res 2003;290:332–45.
39. Soeda A, Park M, Lee D, et al. Hypoxia promotes expansion of the CD133-positive glioma stem cells through activation of HIF-1α. Oncogene 2009;28:3949–59.
40. Saini V, Shoemaker RH. Potential for therapeutic targeting of tumor stem cells. Cancer Sci 2010;101:16–21.
41. Kim JB, Sebastiano V, Wu G, et al. Oct4-induced pluripotency in adult neural stem cells. Cell 2009;136:411–9.
42. Covello KL, Kehler J, Yu H, et al. HIF-2α regulates Oct-4: effects of hypoxia on stem cell function, embryonic development, and tumor growth. Genes Dev 2006;20:557–70.
43. Chang CL, Tsai YC, He L, Wu TC, Hung CF. Cancer immunotherapy using irradiated tumor cells secreting heat shock protein 70. Cancer Res 2007;67:10047–57.
44. Burris HA III, Moore MJ, Andersen J, et al. Improvements in survival and clinical benefit with gemcitabine as first-line therapy for patients with advanced pancreas cancer: a randomized trial. J Clin Oncol 1997;15:2403–13.
45. Garcia-Manteiga J, Molina-Arcas M, Casado FJ, Mazo A, Pastor-Anglada M. Nucleoside transporter profiles in human pancreatic cancer cells: role of hCNT1 in 2',2'-difluorodeoxycytidine-induced cytotoxicity. Clin Cancer Res 2003;9:5000–8.
46. Lam W, Leung CH, Bussom S, Cheng YC. The impact of hypoxic treatment on the expression of phosphoglycerate kinase and the cytotoxicity of troxacitabine and gemcitabine. Mol Pharmacol 2007;72:536–44.
47. Kerbel RS. Tumor angiogenesis. N Engl J Med 2008;358:2039–49.
48. Grunewald M, Avraham I, Dor Y, et al. VEGF-induced adult neovascularization: recruitment, retention, and role of accessory cells. Cell 2006;124:175–89.
49. Gao D, Nolan DJ, Mellick AS, Bambino K, McDonnell K, Mittal V. Endothelial progenitor cells control the angiogenic switch in mouse lung metastasis. Science 2008;319:195–8.
50. Yurugi-Kobayashi T, Itoh H, Yamashita J, et al. Effective contribution of transplanted vascular progenitor cells derived from embryonic stem cells to adult neovascularization in proper differentiation stage. Blood 2003;101:2675–8.
51. Kindler HL, Niedzwiecki D, Hollis D, et al. A double-blind, placebo-controlled, randomized phase III trial of gemcitabine (G) plus bevacizumab (B) versus gemcitabine plus placebo (P) in patients (pts) with advanced pancreatic cancer (PC): a preliminary analysis of Cancer and Leukemia Group B (CALGB) 80303. J Clin Oncol 2007;ASCO Annual Meeting Proceedings Part I. 25(18Suppl1):4508.

GASTROENTEROLOGY 2010;139:882–892

Imbalance of NKp44$^+$NKp46$^-$ and NKp44$^-$NKp46$^+$ Natural Killer Cells in the Intestinal Mucosa of Patients With Crohn's Disease

TETSURO TAKAYAMA,* NOBUHIKO KAMADA,* HIROSHI CHINEN,‡ SUSUMU OKAMOTO,* MINA T. KITAZUME,* JONATHAN CHANG,* YUMI MATUZAKI,§ SADAFUMI SUZUKI,§ AKIRA SUGITA,‖ KAZUTAKA KOGANEI,‖ TADAKAZU HISAMATSU,* TAKANORI KANAI,* and TOSHIFUMI HIBI*

*Division of Gastroenterology and Hepatology, Department of Internal Medicine, §Department of Physiology, Keio University School of Medicine, Tokyo, Japan; ‡Department of Medicine and Therapeutics, Control and Prevention of Infectious Diseases, Graduate School of Medicine, University of the Ryukyus, Nishihara, Japan; ‖Department of Surgery, Yokohama Municipal Citizen's Hospital, Yokohama, Japan;

BACKGROUND & AIMS: Mucosal natural killer (NK) cells that produce interleukin (IL)-22 mediate intestinal homeostasis and inflammation in mice. However, their role in the pathogenesis of human inflammatory bowel diseases (IBDs) is not known. We investigated intestinal NK cells in intestinal mucosa samples of patients with Crohn's disease (CD). **METHODS:** We isolated lamina propria NK cells from intestinal mucosal samples of patients with IBD and subjects without IBD (controls) and analyzed expression patterns of cell surface molecules and cytokine production. Interactions between lamina propria NK cells and intestinal macrophages were examined. **RESULTS:** In intestinal mucosa samples from controls, NKp44 and NKp46 were expressed differentially on CD3$^-$CD56$^+$ NK cells, NKp44$^+$NKp46$^-$ (NKp44$^+$) NK cells expressed CD127 and the transcription factor retinoic acid-related orphan receptor C (RORC) and produced IL-22 whereas NKp44$^-$NKp46$^-$ (NKp46$^+$) NK cells did not express CD127 or RORC and produced interferon (IFN)-γ. NKp46$^+$ NK cells were predominant in intestinal mucosa of patients with CD compared with controls or patients with ulcerative colitis. Upon interaction with intestinal inflammatory macrophages NKp46$^+$, NK cells from patients with CD were activated via IL-23 and produced IFN-γ; this activation required cell-to-cell contact. **CONCLUSIONS: The balance of NKp44$^+$/NKp46$^+$ NK cells is disrupted in intestinal mucosa of patients with CD. NKp46$^+$ NK cells might mediate the pathogenesis of CD by producing IFN-γ.**

Keywords: Intestinal NK Cells; Intestinal Macrophages; UC.

Dysfunction of the mucosal immune system evokes gut inflammation induced by activation of both acquired and innate immunity in inflammatory bowel disease (IBD) including Crohn's disease (CD) and ulcerative colitis (UC).[1–7] Among the innate immune compartments, natural killer (NK) cells appear to participate in the pathogenesis of autoimmune disease,[8–10] including IBD. Furthermore, several groups recently have identified a unique subset of mucosal NK cells in both human beings and mice that contributes to local mucosal immunity, including in the gut mucosa.[11–15] These mucosal NK cells are distinct from conventional NK cells, and are characterized by their expression of a transcription factor, RORC in human or RORγt in mice, CD127 (interleukin [IL]-7Rα) and NKp44 in human beings or NKp46 in mice. Moreover, these newly identified NK cells produce IL-22.[11] However, it is still controversial whether these IL-22–producing NK cells participate in pathologic or protective processes of chronic inflammation in vivo. In human beings, CD56$^+$CD127$^+$ NK cells are generated from lymphoid tissue-inducer (LTi) cells and produce little interferon (IFN)-γ, whereas CD56$^+$CD127$^-$ NK cells produce a large amount of this cytokine.[13] The results of a mouse study also suggested that mucosal IL-22–producing RORγt$^+$ NK cells are derived from LTi cells and that commensal bacteria are needed for their development.[11,15]

Controversially, however, some recent previous reports suggested that 2 NK activation markers, NKp44 and NKp46, are expressed differently in mice and human beings, and that NKp44$^+$NK cells correspond to human mucosal NK cells (NK-22 cells) and NKp46$^+$ NK cells correspond to rodent NK-22 cells. However, other groups have reported that NK-22 cells in human beings are also NKp46$^+$ cells, showing by immunohistochemistry[12] and unpublished data[8] that the NKp46$^+$ cells reside in human gut, although their function in the gut is not proven.[12] Therefore, we wondered whether NKp44$^+$ cells and NKp46$^+$ cells were the same population, that is, do NK-22 cells express both NKp44 and NKp46? Accumulating data suggest differences in the immune mecha-

Abbreviations used in this paper: **CD, Crohn's disease; IBD, inflammatory bowel disease; IFN, interferon; IL, interleukin; LP, lamina propria; LPMC, lamina propria mononuclear cell; LPNK, lamina propria natural killer cells; LTi, lymphoid tissue-inducer cells; mAb, monoclonal antibody; Mϕ, macrophage; NC, normal control; NK, natural killer; PBNK, peripheral blood natural killer cells; PCR, polymerase chain reaction; RT, reverse transcription; TL1A, TNF-like cytokine 1A; TNF, tumor necrosis factor; UC, ulcerative colitis.**

0016-5085/$36.00
doi:10.1053/j.gastro.2010.05.040

nisms of mice and human beings. Because of these issues, it is necessary to assess human gut samples and human gut mucosal NK cells in particular to evaluate their role in the pathogenesis of several human diseases, including IBD.

We previously identified similar precursors of lamina propria (LP) NK cells in human intestine. These cells show the c-kit+ lineage marker, an LTi cell-like phenotype, and give rise to CD56+c-kit^{dim} LPNK cells.[16] We also reported that the local differentiation of NK cells was augmented in patients with CD, and therefore the percentage of LPNK cells increased in CD. It also has been reported that NK cells produce IFN-γ through cross-talk with surrounding cells such as dendritic cells.[17-20] Our group and others have reported that IFN-γ plays an important role in the pathogenesis of CD.[5,6,21,22] Hence, it is possible that LPNK cells, whose number increases in patients with CD, play an important role in intestinal inflammation through the increased production of IFN-γ.

It recently has become evident that macrophages (Mϕs) also play important roles in maintenance of homeostasis,[23-26] and we have shown that human LPMϕs play a key role in the innate immune response against commensal bacteria.[27] We identified a unique subset of LPMϕs whose numbers increase in CD patients. This subset expresses both the Mϕ marker CD14 and dendritic cell marker CD209, and produces robust amounts of IL-23 in response to stimulation with commensal bacteria.[27] Because it has been reported that mucosal NK cells are stimulated by IL-23,[13] we logically hypothesized that the CD14+LPMϕs might activate LPNK cells through IL-23 signaling and be involved in the pathogenesis of CD. In the present study, we focused on the role of LPNK cells, and attempted to clarify the role of the cross-talk between LPNK cells and CD14+LPMϕs in the pathogenesis of CD.

Materials and Methods

Tissue Samples

Normal intestinal mucosa was obtained from macroscopically and microscopically unaffected areas of patients with colon cancer.

Intestinal mucosa (large intestine) was obtained from surgically resected specimens from patients with UC or CD who were diagnosed on the basis of clinical, radiographic, endoscopic, and histologic findings according to established criteria. In all samples the degree of inflammation was histologically moderate to severe. All experiments were approved by the institutional review board in all institutions, and written informed consent was obtained from all patients.

Histologic Analysis

Tissue sections were treated according to established methods as reported previously.[16] Anti-CD3 monoclonal antibody (mAb), anti-CD56 mAb (MOC-1), or anti-IFN-γ mAb (25718) were purchased from Dako (Glostrup, Denmark). Secondary antibody conjugated to Alexa Fluor 350, 488, or 566 were from Molecular Probes (Eugene, OR).

Preparation of Lamina Propria Mononuclear Cells

Lamina propria mononuclear cells (LPMCs) were isolated from intestinal specimens using modifications of previously described methods.[28]

Isolation of CD3−CD56+ NKp44+NKp46− and NKp44−NKp46+ NK Cells

Whole LPMCs from normal controls (NCs) were stained and dead cells were excluded with propidium iodide staining. Stained cells were isolated with Moflo (Dako) according to the manufacturer's instructions. In isolation of LPNK cells from CD, CD3− CD56+ cells were isolated with Moflo. The percentage of NKp44−NKp46+ cells was routinely greater than 90%.

Isolation of LP CD14+ Macrophages

CD14+LPMϕs were isolated from LPMCs using Human CD14+ EasySep (Stemcell Technologies, Inc Vancouver, BC, Canada) according to the manufacturer's instructions. The percentage of each isolated CD14+LPMϕ was routinely greater than 95%.

Flow Cytometry

The cell surface fluorescence intensity was assessed using a FACSCalibur analyzer (BD Pharmingen (San Diego, CA) and analyzed using CellQuest software (BD Biosciences, San Jose, CA) or FlowJo (TreeStar (Ashland, OR)). Dead cells were excluded with propidium iodide staining. The mAb to CD56 was purchased from BD Biosciences. The mAbs to CD3 were from eBioscience (San Diego, CA). Abs to CD69, CD122, and CD244 were from BD Biosciences. The mAbs to NKp46, NKp44, NKp46, and CD127 were from Beckman-Coulter (Brea, CA). The mAbs to NKG2D were from eBioscience. mAb to IL-15 was from R&D Systems (Minneapolis, MN), to IL-18 from MBL (Nagoya, Aichi), to IL-12p40/p70 from eBioscience, and to tumor necrosis factor (TNF)-like cytokine 1A (TL1A) from BioLegend (San Diego, CA). Human recombinant IL-23 and TL1A were from R&D Systems.

NK Cell Cytokine Production

Measurement of IFN-γ and TNF-α production from intestinal NK cells was performed by using Cytokine Secretion Assays Detection Kits (Miltenyi Biotec, Gladbach, Germany) according to the manufacturer's instructions.

Intracellular Cytokine Staining

For intracellular staining, whole LPMCs were stimulated with IL-23 (20 ng/mL) or commensal bacterial anti-

gen (*Escherichia coli* [100 multiplicities of infection (MOI)] or *Enterococcus faecalis* [100 MOI]) for 9 hours and in the presence of monensin (Golgistop; BD Pharmingen) for another 4 hours. After the stimulation, a Cytofix/Cytoperm Kit (BD Pharmingen), anti-CD3 mAb (BD PharMingen), anti-IL-17 mAb (eBioscience), and anti-IL-22 mAb (eBioscience) were used according to the manufacturer's instructions.

Commensal Bacterial Heat-Killed Antigens

E coli (catalogue no. 25922; ATCC) and *E faecalis* (ATCC29212) were used as reported previously.[27]

Quantitative Real-Time Reverse-Transcription Polymerase Chain Reaction Analysis

Total RNA was extracted using an RNeasy Micro Kit (Qiagen, Hilden, Germany), and cDNA was synthesized using a Quantitect reverse-transcription (RT) kit (Qiagen), according to the manufacturer's instructions. Quantitative real-time RT-polymerase chain reaction (PCR) was performed using a TaqMan universal PCR master mix (Applied Biosystems, Foster City, CA) and on-demand gene-specific primers, assessed using the DNA Engine Opticon 2 system, and analyzed with Opticon monitor software (MJ Research, Waltham, MA). The primers were as follows: *IL12p35* (Hs00168405), *IL12p40* (Hs00233688), *IL23p19* (Hs00372324), *IL15* (Hs01003716_m1), *IL18* (Hs00155517_m1), *RORC* (Hs01076112_m1), *IL23R* (Hs00332759_m1), *TNFSF15* (Hs00353710_s1), *IL22* (Hs00220924_a1), *IFNg* (Hs00174143_a1), and *ACTB* (Hs99999903). All primers were purchased from Applied Biosystems. Relative quantification was achieved by normalizing to the values of the *Actb* gene.

Cytokine Assay

Human inflammation or a T-helper (Th)1/Th2-II cytometric beads array kit (BD Pharmingen) was used for cytokine measurements and tests were performed according to the manufacturer's instructions.

Statistical Analysis

Statistical analysis was performed using GraphPad Prism software version 4.0 (GraphPad Software, Inc, San Diego, CA). A P value of less than .05 was regarded as significant. All data are expressed as mean ± standard error of the mean.

Results

Two Different Types of NKp44$^-$NKp46$^+$ and NKp44$^+$NKp46$^-$ NK Cells Reside in Human Intestinal Mucosa

We first precisely analyzed the phenotype of LP NK (hereafter called *LPNK*) cells as well as peripheral blood NK (PBNK) cells in NCs. As shown in Figure 1*A*, we found that CD3$^-$CD56$^+$ PBNK cells obtained from normal individuals seem to be homogenous, and strongly express NKp30, NKp46, CD122 (IL-15Rβ), NKG2D, and CD244, but not NKp44, CD127 (IL-7Rα), and CD69, suggesting that PBNK cells are IL-15–dependent conventional NK cells. In contrast, CD3$^-$CD56$^+$ LPNK cells were quite heterogeneous, some expressing each of NKp30, NKp44, NKp46, CD122, CD127, NKG2D, and CD244, but almost all cells expressing CD69 (Figure 1*A*). According to previous reports, mucosal NK cells express CD69,[16] intestinal LPNK cells have similar phenotypes in cell surface marker use. To assess the relationship further between expressions of each molecule in LPNK cells, we counterstained pairs of molecules in addition to CD3 and CD56. To our surprise, NKp44 and NKp46 molecules were expressed differentially on CD3$^-$CD56$^+$ LPNK cells, and NKp44$^+$NKp46$^+$ double-positive LPNK cells were very rare (Figure 1*B*). Furthermore, NKp44$^+$NKp46$^-$ LPNK cells (so-called *NKp44$^+$ NK* cells) expressed CD127 but not CD122, whereas NKp44$^-$NKp46$^+$ LPNK cells (so-called *NKp46$^+$ NK* cells) expressed CD122 but not CD127 (Figure 1*B*). To examine further which subpopulation expresses RORC, IL-22, IFN-γ, and IL-23R, we performed an RT-PCR assay. As shown in Figure 1C, messenger RNAs (mRNAs) of both RORC and IL-22 were expressed preferentially in NKp44$^+$ NK cells, whereas mRNA of IFN-γ was present in the NKp46$^+$ NK cell population. Both NKp44$^+$ and NKp46$^-$ NK cells expressed IL-23R whereas PBNK cells were not (Figure 1C and data not shown). Collectively, human intestinal NK cells were distinct from PBNK cells and divided into 2 populations, represented by the NKp44$^+$NKp46$^-$ (similar subset to NK-22 cells, which was reported previously in human tonsil) and NKp44$^-$NKp46$^+$ populations, respectively.

LPNK Cells Are a Major Source of IFN-γ and Are Involved in the Pathogenesis of CD

We next assessed the role of LPNK cells in the immunopathology of IBD. As we previously reported,[16] the proportion of CD3$^-$CD56$^+$ LPNK cells was increased significantly in CD patients compared with that in NCs or patients with UC (Figure 2*A*). Because we and others previously have reported that IFN-γ plays an important role in the pathogenesis of CD,[21] we hypothesized that LPNK cells are major producers of IFN-γ in addition to CD3$^+$ T cells. As expected, immunohistochemical examination revealed that the number of IFN-γ–expressing CD3$^-$CD56$^+$ LPNK cells was increased markedly in inflamed mucosa of CD compared with NC and UC patients (Figure 2*B*). Moreover, in CD, we found that the ratio of IFN-γ–expressing CD3$^-$CD56$^+$ LPNK cells was increased markedly in response to commensal bacterial antigens (*E faecalis* [Figure 2C] and *E coli* [Supplementary Figure 1]), whereas IL-17 was produced in response to living bacteria by CD3$^+$ T, but not CD3$^-$CD56$^+$ NK cells (Figure 2C and Supplementary Figure 1).

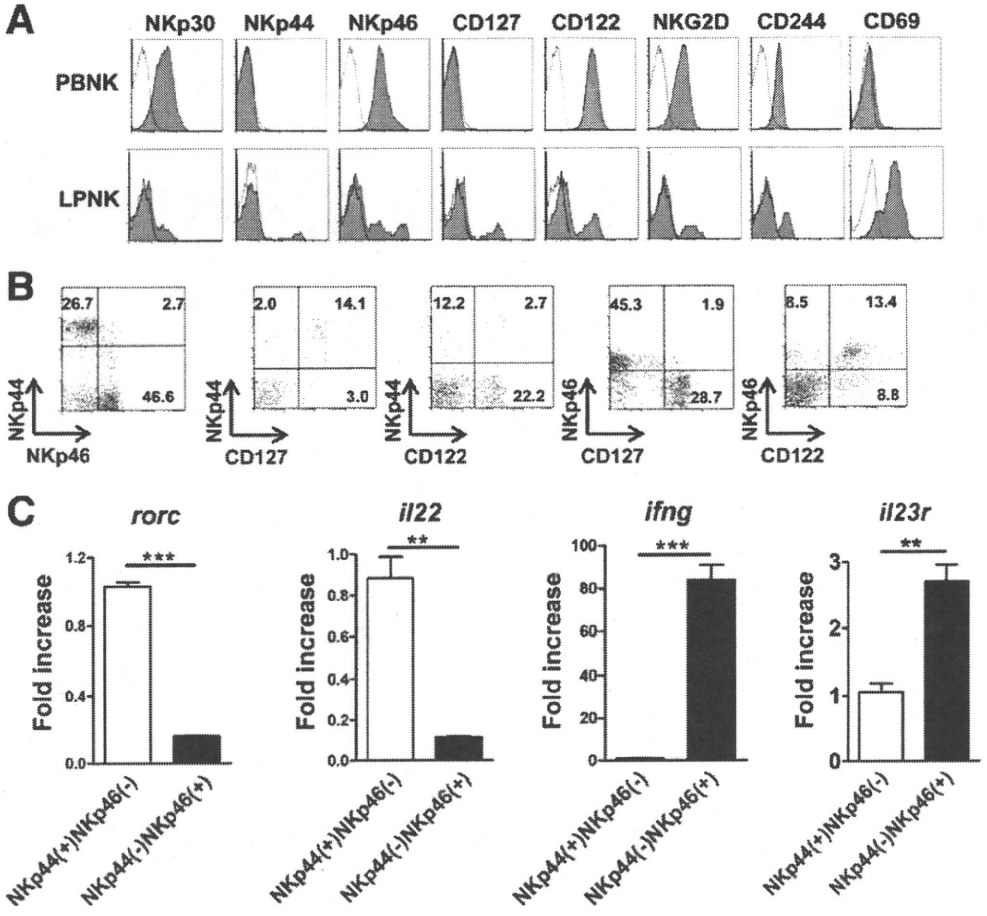

Figure 1. NKp44+NKp46− and NKp44−NKp46+ NK cells produce IL-22 and IFN-γ, respectively. (*A*) Cell surface molecules of LPNK cells and PBNK cells of NC. The open histograms show the isotype control and the filled histograms show the indicated surface molecules ($n = 5$). (*B*) Expression of NKp44 and NKp46 or CD127 and CD122 on LPNK cells from NCs was examined. (*C*) The expression level of the indicated mRNA of isolated NKp44+NKp46− and NKp44−NKp46+ NK cells were measured. $^{**}P < .005$; $^{***}P < .0001$.

IFN-γ–Producing NKp46+ NK Cells Preferentially Reside in Inflamed Mucosa of CD

The aforementioned experiments showed that CD3−CD56+ LPNK cells of CD patients produce large amounts of IFN-γ. We next precisely characterized by flow cytometry LPNK cells of CD patients in parallel with those of UC patients or NCs. First, we confirmed whether NKp44 and NKp46 molecules were expressed differentially on CD3−CD56+ LPNK cells of IBD patients and NCs. Strikingly, the proportion of NKp44+ NK cells was decreased significantly in CD compared with UC and NC patients, while conversely the proportion of NKp46+ NK cells was increased significantly in CD compared with UC and NC patients (Figure 3). No significant differences in these proportions were observed between NC and UC patients (Figure 3). Furthermore, almost all LPNK cells of CD patients preferentially expressed NKp30, CD122, NKG2D, and CD244 (Figure 3*A*), suggesting that LPNK cells of CD predominantly are NKp46+ NK cells, not NKp44+ NK cells.

Given the evidence that the major population of LPNK cells is NKp46+ NK cells, we next stimulated isolated LPMCs with *E faecalis* or *E coli* in vitro, and assessed the production of IFN-γ and TNF-α by NKp46+ NK or NKp44+ NK cell populations. Similarly to LP, NKp46+ NK cells obtained from NC and IBD patients produced IFN-γ (Figure 4), and the proportion of IFN-γ–producing NKp46+ NK cells in CD was significantly higher compared with NC. In UC, the ratio of IFN-γ–expressing NKp46+ NK cells also significantly was increased compared with NC, and tended to be lower than that of CD, but the difference was not significant (Figure 4). In all groups, NKp44+ NK cells produce IL-22 (data not shown). In contrast to IFN-γ and IL-22, both NKp46+ and NKp44+ NK cells produced TNF-α in response to commensal bacterial stimulation in all groups, suggesting that the different molecular mechanism of stimulation lies in the signal pathway (Supplementary Figure 2).

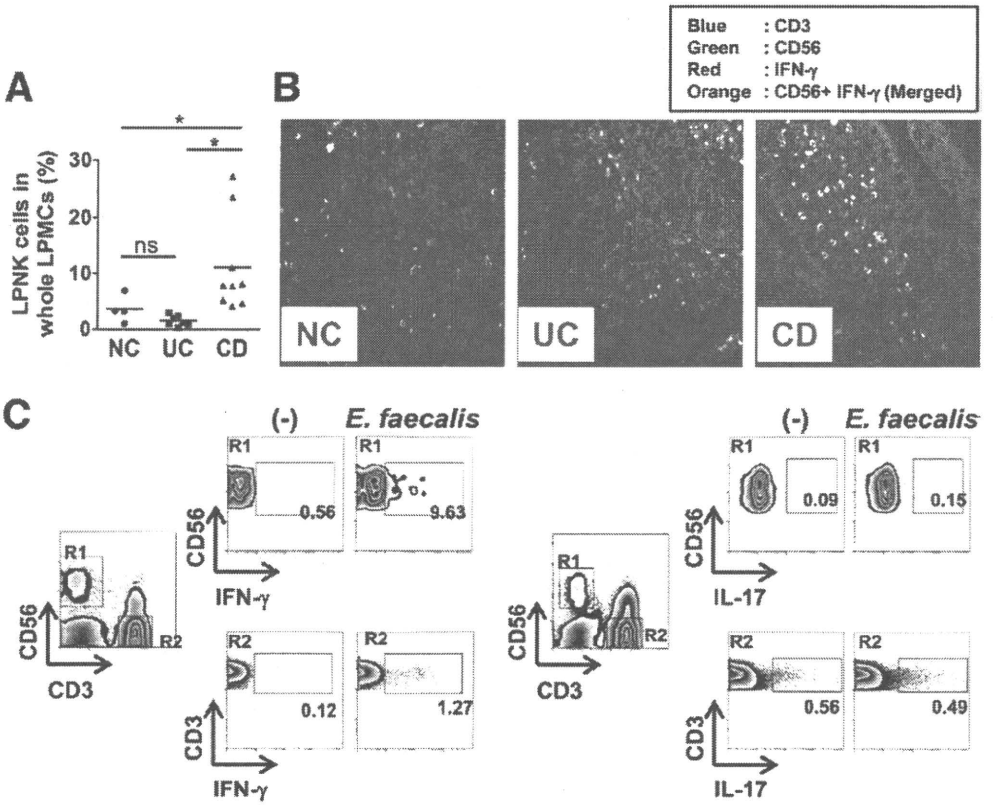

Figure 2. IFN-γ–producing $CD3^-CD56^+$ LPNK cells are increased in the inflamed mucosa of CD patients. (*A*) The percentage of $CD3^-CD56^+$ LPNK cells in CD is increased significantly compared with UC or NC (NC, 4; UC, 7; CD, 9). $^*P < .05$. (*B*) Intestinal mucosa specimens from NC and patients with UC or CD were stained. Original magnification, 100×. (*C*) IFN-γ was produced mainly by $CD56^+CD3^-$ LPNK cells rather than $CD56^-CD3^+$ T cells in response to stimulation with commensal bacterial antigen. R1 represents the NK cell population and R2 T cells. One representative experiment of 5 independent experiments is shown.

BASIC—ALIMENTARY TRACT

IFN-γ Production by LPNK Cells Requires an Interaction With $CD14^+$LPMϕs

The aforementioned results suggest to us that intestinal IFN-γ–producing $NKp46^+$ NK cells were increased dramatically in the intestinal mucosa of CD patients, and the IFN-γ production by LP $NKp46^+$ cells was induced with the stimulation of commensal bacteria antigens. Thus, we wondered whether intestinal $NKp46^+$ NK cells could produce IFN-γ in direct response to stimulation with commensal bacteria or via cross-talk with surrounding cells. As we previously reported,[27] inflammatory $CD14^+$LPMϕs are increased dramatically in inflamed mucosa of CD and play a critical role in commensal bacteria-triggered inflammatory responses in the intestinal mucosa. Thus, it is possible that an interaction between intestinal $NKp46^+$ NK cells and $CD14^+$LPMϕs is critically involved in the production of IFN-γ by intestinal $NKp46^+$ NK cells. Therefore, we first examined whether the production of IFN-γ from intestinal $NKp46^+$ NK cells is retained after depletion of $CD14^+$LPMϕs from LPMCs of CD patients. As shown in Figure 5*A* and *B*, IFN-γ production by intestinal $NKp46^+$ NK cells in response to *E faecalis* stimulation was abolished by depleting $CD14^+$ cells, suggesting that an interaction between $CD14^+$ LPMϕs and intestinal $NKp46^+$ NK cells is needed to activate intestinal $NKp46^+$ NK cells to produce IFN-γ. Of note, LPNK cells did note express TLR2 or TLR4 (data not shown). TNF-α production by LPNK cells in response to *E faecalis* also was reduced by depleting $CD14^+$ cells (Supplementary Figure 3).

IL-23 and TL1A Produced by $CD14^+$LPMϕs and Direct Cell-to-Cell Interaction Are Needed to Activate LPNK Cells

Finally, we addressed the mechanism of the interaction between $CD14^+$LPMϕs and intestinal $NKp46^+$ NK cells for IFN-γ production in CD. First, we examined whether soluble factors (cytokines) produced by $CD14^+$LPMϕs can stimulate intestinal $NKp46^+$ NK cells. To this end, we used a quantitative RT-PCR assay to identify the cytokines produced by $CD14^+$LPMϕs in response to *E faecalis*. *E faecalis* stimulation strongly induced IL-23p19 and IL-12p40 expression, but these were reduced significantly by depleting $CD14^+$LPMϕs from LPMCs (Figure 5*C*). In contrast, other candidate soluble factors, such as IL-12p35, IL-15, and IL-18, were not induced by the same stimulation and

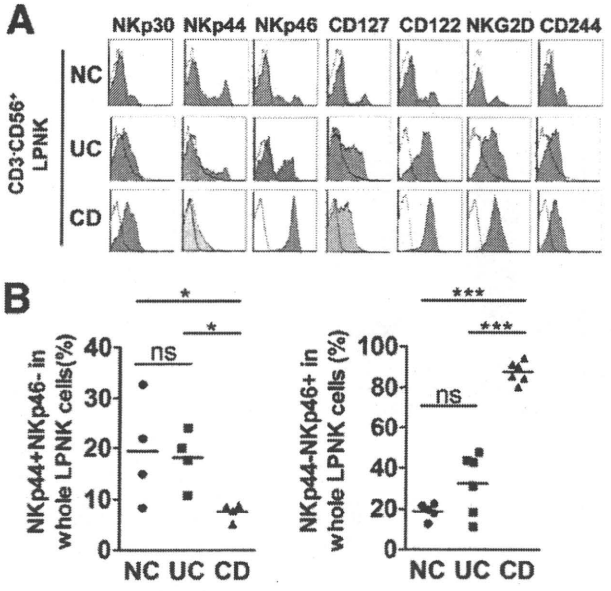

Figure 3. The proportion of NKp44$^-$NKp46$^+$ LPNK cells in total LPNK cells is increased abnormally in CD. (*A*) Cell surface molecules of LPNK cells from NCs and patients with UC or CD (n = 5). (*B*) Left: percentage of NKp44$^+$NKp46$^-$ cells per total CD56$^+$ CD3$^-$ LPNK cells. Right: percentage of NKp44$^-$NKp46$^+$ cells per CD56$^+$ CD3$^-$ LPNK cells (NC, 5; UC, 6; CD, 6). *$P < .05$; ***$P < .0001$.

were not affected by depleting CD14$^+$ cells (Figure 5*C*). This was also the case after stimulation by *E coli* (data not shown). Collectively, these data suggest that commensal bacteria stimulate CD14$^+$LPMϕs to preferentially produce IL-23 (IL-23p19/IL-12p40), but not IL-12 (IL-23p35/IL-12p40), IL-15, or IL-18.

Given the evidence that IL-23, but not IL-12, IL-15, or IL-18, specifically was induced in CD14$^+$LPMϕs of CD by commensal bacteria stimulation, we further assessed the effect of those cytokines by addition of neutralizing mAbs. Notably, the addition of neutralizing anti-IL-12/23p40 mAb, but not anti-IL-15 or anti-IL-18 mAb, to LPMCs from CD patients cultured with *E faecalis* dramatically reduced IFN-γ production in intestinal NKp46$^+$ NK cells (Figure 5*D* and *E*). Next, we assessed the direct cell-to-cell interaction between CD14$^+$LPMϕs and NKp46$^+$NK cells using the transwell culture system (Figure 6*A* and *B*). IFN-γ production by intestinal NKp46$^+$ NK cells was greatly reduced by inhibiting their direct cell-to-cell interaction with CD14$^+$LPMϕs. This result suggests direct cell-to-cell interaction with CD14$^+$ LPMϕs also was required for activation of NKp46$^+$ NK cells.

To further confirm the earlier-described results, we used isolated LPNK cells and CD14$^+$LPMϕs and performed the similar co-culture experiments. Consistent with the former results, LPNK cells produced IFN-γ in both protein and mRNA level only if they co-cultured with LPMϕs. Moreover, this LPNK cell activation by LP Mϕs was dependent on cell-to-cell contact and IL-23, which was produced by LPMϕs in response to *E faecalis* stimulation (Figure 6*C* and *D*).

To assess further the possibility that IL-23 alone without cell-to-cell contact can activate intestinal NKp46$^+$ NK cells of CD to produce IFN-γ, we administered recombinant IL-23 to cultures of CD14$^+$ cell-depleted LPMCs, but only a small amount of IFN-γ production by intestinal NKp46$^+$ NK cells was induced in these cultures compared with those stimulated with commensal bacteria (Figure 7*A* and *B*). Dose escalation of IL-23 did not induce an increase of IFN-γ by NKp46$^+$ NK cells (Supplementary Figure 4). These data suggest that although

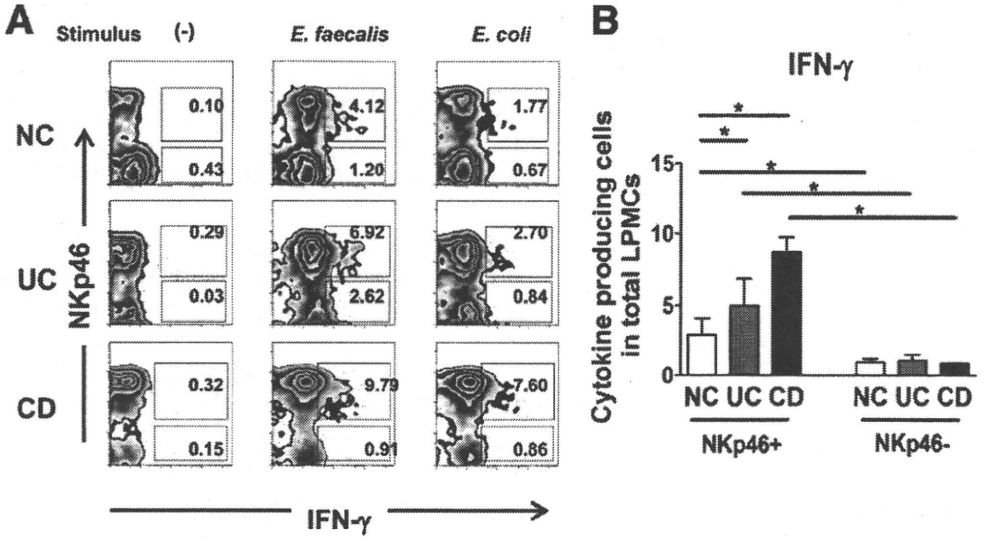

Figure 4. NKp44$^-$ NKp46$^+$ NK cells produce large amounts of IFN-γ by stimuli of commensal bacterial antigen. (*A*) LPNK cells from NCs or patients with UC or CD were stimulated with the commensal bacterial antigen. IFN-γ expression in the indicated cell populations was measured ($n = 5$). (*B*) Statistical analysis of IFN-γ expression in the indicated cell populations. *$P < .05$.

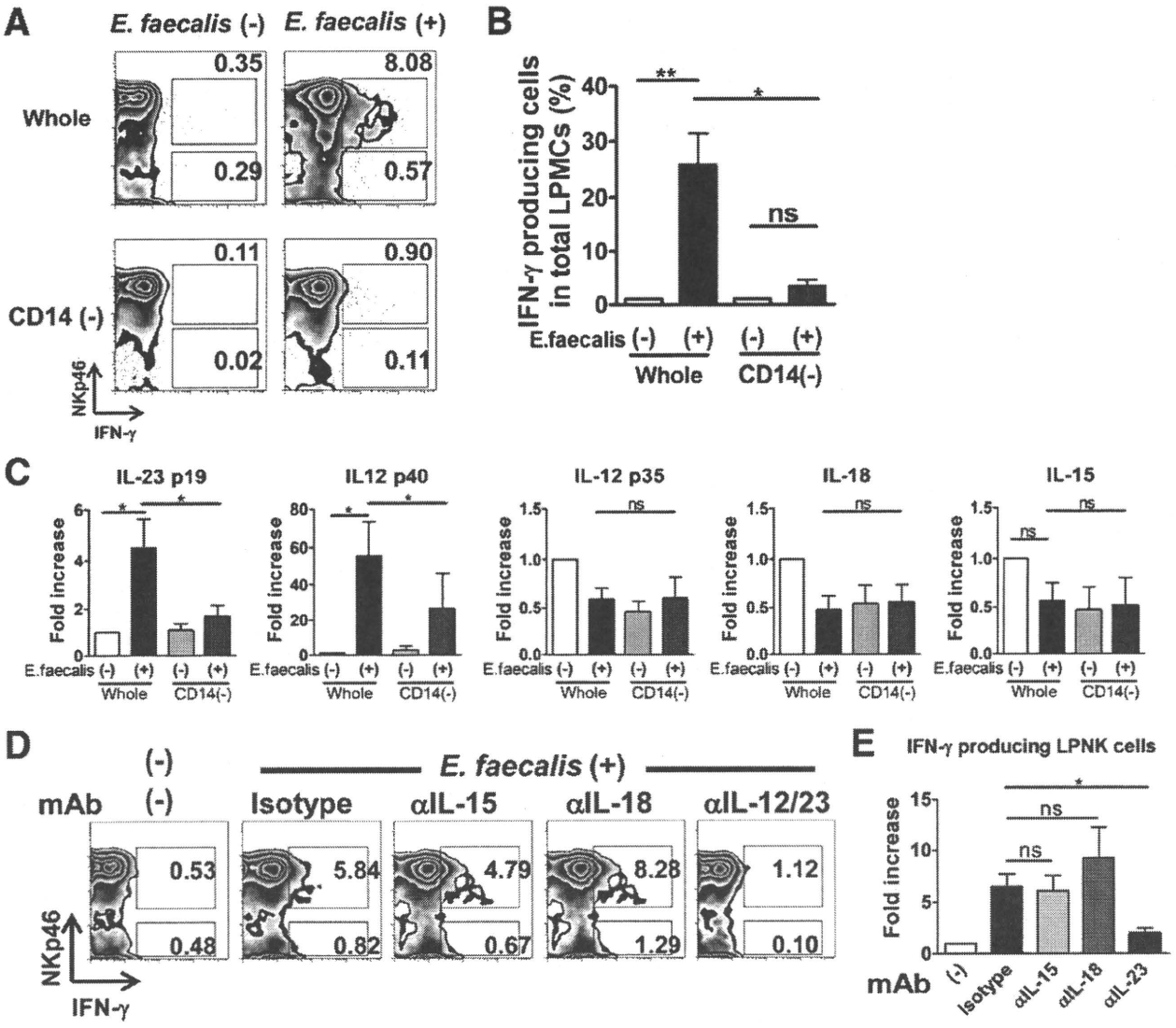

Figure 5. IFN-γ expression in NKp44$^-$NKp46$^+$ LPNK cells in response to stimulation with commensal bacteria antigen is abolished by the depletion of CD14$^+$ LPMϕs. (A) IFN-γ expression in the indicated cell populations was measured (n = 3). (*B*) The fold increase in the percentage of IFN-γ–positive LPNK cells (whole LPMCs, n = 9; CD14$^+$ cell-depleted LPMCs, n = 3). IL-23 is the key molecule for the interaction of CD14$^+$ Mϕs and LPNK cells. (*C*) IL-23, but not IL-15 or IL-18, is induced in CD14$^+$ LPMϕs from patients with CD in response to *E faecalis* stimulation. Quantitative RT-PCR of mRNA expression levels (n = 5). (*D*) Neutralization of IL-23, but not IL-15 or IL-18, reduced IFN-γ production from LPNK cells in response to *E faecalis* stimulation (n = 3). (*E*) Statistical analysis of the percentage of IFN-γ–producing cells in LPNK cells was performed (n = 3). *P < .05; P < .005.

IL-23 is required to induce IFN-γ by intestinal NKp46$^+$ NK cells of CD patients, additional soluble factors and/or cell-to-cell contact with CD14$^+$ LPMϕs also are required.

CD has been reported to be associated with variations in the gene encoding the IL-23R subunit. Similarly, a possible association of CD with a TNF-α family member, TL1A, which is produced by or expressed on various antigen-presenting cells, recently was reported. We previously reported that TL1A cooperatively acts with IL-23, and synergistically induces Th1 and Th17 responses on T cells.[29] Thus, we assessed the involvement of TL1A molecules in the cell-to-cell interaction required for LPNK-derived IFN-γ induction. Consistent with our previous findings, TL1A mRNA was expressed in CD14$^+$ cells obtained from inflamed mucosa of CD, and was upregulated markedly by bacterial antigen stimulation (Supplementary Figure 5). Of note, IFN-γ production from intestinal NKp46$^+$ NK cells was inhibited significantly by the addition of neutralizing anti-TL1A mAb, although the effect was partial (Figure 7*C* and *D*). Furthermore, the proportion of IFN-γ–expressing intestinal NKp46$^+$ NK cells from CD patients in culture was increased significantly by the addition of a mixture of

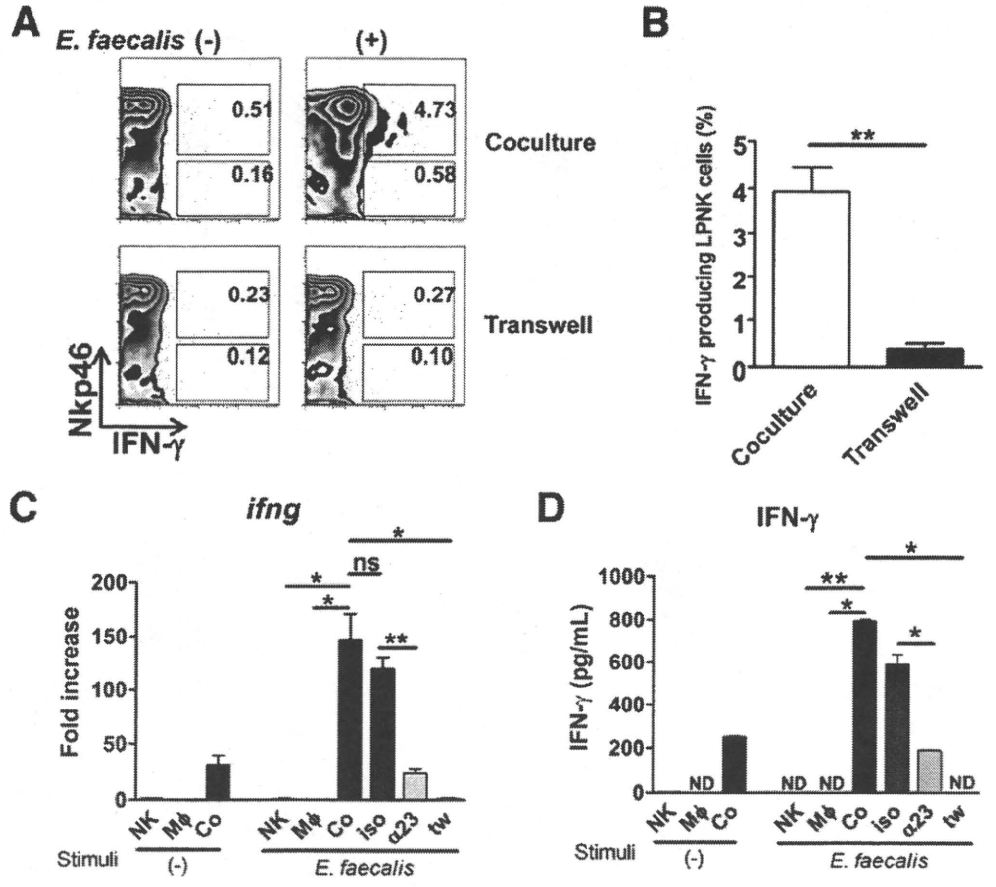

Figure 6. Direct cell-to-cell interaction between LPNK cells and LP CD14+ Mϕs is required to produce IFN-γ in response to commensal bacteria stimulation. (*A*) IFN-γ production was evaluated in a co-culture or transwell culture of CD14+ cells isolated from LPMC and CD14+ cell-depleted LPMC. Upper panels: co-culture. Lower panels: transwell. One representative experiment of 3 independent experiments is shown. (*B*) Statistical analysis of the percentage of IFN-γ–producing cells in LPNK cells was performed ($n = 3$). Intestinal NK cells produce IFN-γ via cross-talk with intestinal Mϕs in CD. IFN-γ production of isolated LPNK cells and CD14+ LPMϕs were measured. (*C*) Quantitative RT-PCR of mRNA expression levels (*D*) protein levels. Data of triplicate samples (1 representative of 3 independent experiments with similar results) are given as mean ± standard deviation. Co, co-culture. $^*P < .05$; $^{**}P < .005$.

recombinant IL-23 and TL1A compared with stimulation with IL-23 or TL1A alone (Figure 7*E* and *F*). These results suggested that TL1A might be a molecule involved in the interaction between LP NK cells and LP Mϕs to induce robust production of IFN-γ.

Discussion

In the present study, we showed that most human LPNK cells are divided into 2 populations: IFN-γ–producing NKp46+ NK cells (CD3−CD56+NKp44−NKp46+ $RORC^{dull}CD122^+CD127^-$) and IL-22–producing NKp44+ NK cells (CD3−CD56+NKp44+NKp46− $RORC^{high}CD122^-$ CD127+). Interestingly, intestinal IFN-γ–producing NKp46+ cells were increased significantly in inflamed mucosa of CD whereas IL-22–producing NKp44+ cells were reduced markedly. Moreover, IFN-γ production by LP NKp46+ cells of CD patients is regulated closely by their interaction with the surrounding LPMϕs in a manner dependent on both LPMϕ production of IL-23 and cell-to-cell contact, including the involvement of TL1A.

Recent intensive reports have reported that mucosal tissues have a unique NK cell subset, so-called *mucosal NK cells*, in both human beings and mice.[11–15] Mucosal NK cells in human beings are identified as an expression of a transcription factor RORC, surface molecules CD127 (IL-7Rα), and NKp44 expression and production of IL-22, but not IFN-γ.[11–15] Importantly, this mucosal-specific NK cell subset is developed locally in mucosal tissues from their precursors, such as c-kit+CD127+RORγt+ LTi cells in murine intestine and lin− c-kit+CD127+RORC+ LTi-like cells in human tonsil.[30] Herein, we showed that the IL-22–producing NKp44+ mucosal NK cell subset was decreased in the inflamed mucosa of CD patients, whereas IFN-γ–producing NKp46+ NK cells were increased dramatically. Importantly, our previous report showed that the IFN-γ–producing LP NK cell subset

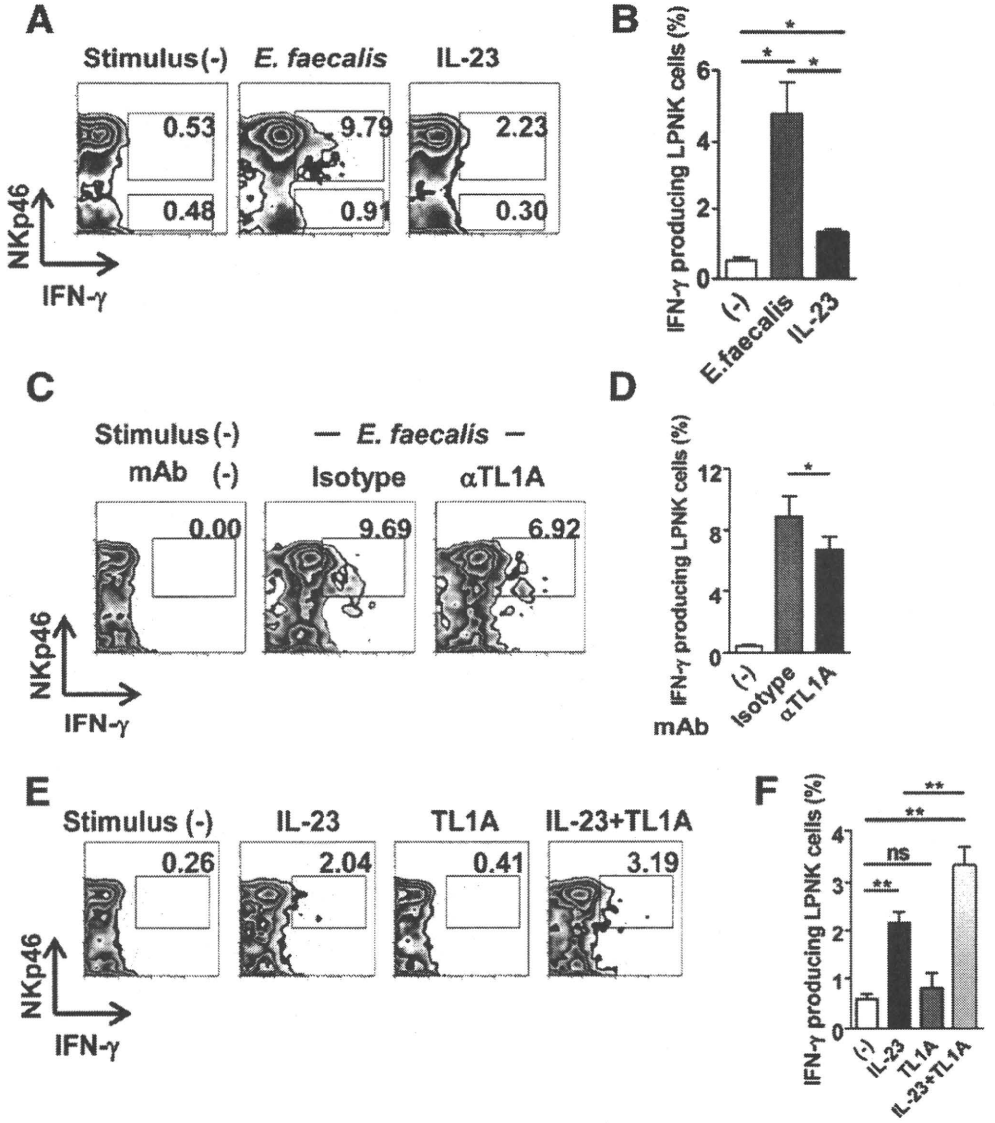

Figure 7. IL-23 and TL1A synergistically activate LPNK cells. (*A*) IL-23 activates LPNK cells to induce a small but substantial IFN-γ expression. IFN-γ expression in the indicated cell populations was measured ($n = 3$). (*B*) Statistical analysis of the percentage of IFN-γ–producing cells in LPNK cells was performed ($n = 3$). (*C*) Inhibition of TL1A slightly but significantly decreased IFN-γ expression in LPNK cells ($n = 3$). (*D*) Statistical analysis of the percentage of IFN-γ–producing cells in LPNK cells was performed (n = 3). (*E*) Addition of a mixture of recombinant IL-23 and TL1A synergistically activates LPNK cells ($n = 3$). (*F*) Statistical analysis of the percentage of IFN-γ–producing cells in LPNK cells was performed ($n = 3$). All statistical data were analyzed using a paired *t* test. *$P < .05$; ** $P < .005$.

locally gave rise from lin$^-$ c-kit$^+$CD127$^+$ LTi-like NK cell precursors in human intestinal mucosa, and this local differentiation of IFN-γ–producing NK cells are accelerated in inflamed mucosa of CD patients compared with NC and UC patients.[16] Collectively, IFN-γ–producing NKp46$^+$ NK cells and IL-22–producing NKp44$^+$ cells might have the same origin, and balance between the developments of these 2 mucosal NK cell subsets may play an important role in the intestinal inflammation of CD.

Meanwhile, it recently was reported that IL-22 plays a protective role in intestinal inflammation. IL-22–producing T cells, NK cells, and dendritic cells were important for the protection from murine adaptive transfer colitis and dextran sulfate sodium (DSS) colitis.[31,32] In addition, overexpression of IL-22 protected the onset of murine colitis.[33] Moreover, a recent study showed the relevance of IL-22–receptor polymorphisms in the incidence of IBD.[34,35] Thus, it is possible that a decreased number of IL-22–producing NKp44$^+$ NK cells in intestinal mucosa led to impaired protective function against intestinal inflammation in CD patients.

On the other hand, previous studies also showed a significant increase of IL-22 production in inflamed mu-

cosa of CD patients,[34] albeit the role of IL-22 whether protective or inflammatory is still poorly understood in human IBD. In addition to the mucosal NK cell subset, it was reported that Th17 cells or dendritic cells produce IL-22.[31,32] More recently, a novel IL-22–producing T-cell subset, so-called *Th22 cells*, are identified in human skin.[36] Thus, it is possible that these cells contributed to the increased production of IL-22 in inflamed mucosa of CD patients despite the fact that IL-22–producing NKp44+ mucosal NK cells were much less prevalent in CD patients. Although the role of IL-22 in IBD pathogenesis should be clarified more closely, it might be involved in the pathogenesis of CD.

Our previous report suggested that IFN-γ production correlates more closely with the pathogenesis of CD than it does with UC.[21] Given that to date IFN-γ has been thought to be produced mainly by LP CD3+ T cells, especially Th1-type CD3+CD4+ T effector cells, it has become evident that the NKp46+ mucosal NK cell subset may be one of the major sources of IFN-γ in inflamed mucosa of CD patients in addition to T cells. Moreover, importantly, the present study clearly showed that the intestinal inflammatory Mϕ subset was important for the activation of LPNK cells to produce IFN-γ. Emerging evidence suggests that NK cells can interact with dendritic cells and Mϕs in physiologic and pathologic conditions.[17–20] For instance, it is known that they can interact with Kupffer cells in liver[18] and uterine Mϕs.[19] Until now, the importance of IL-12, IL-15, and IL-18 has been highlighted in the interaction between NK cells and Kupffer cells.[18] However, IL-23 is a newly identified inflammatory cytokine whose role is in the development and maintenance of Th17-type CD4+ T cells.[37,38] In our present study, however, inhibiting the IL-23 signal greatly reduced IFN-γ production by intestinal NKp46+ NK cells (Figure *5D* and *E*). To our surprise, because large amounts of IL-23, but not IL-12, IL-15, or IL-18, were produced from CD14+LPMϕs of CD in response to stimulation with commensal bacteria (Figure *5C* and our previous observation[27]), IL-23 preferentially may be involved not only in Th17 cells, but also in LPNK cells, to induce IFN-γ production as a key mediator in gut-specific inflammation. Consistent with this finding, Hue et al[37] recently showed that T-cell–deficient RAG-1$^{-/-}$ mice infected with *Helicobacter hepaticus* developed innate immune cell-mediated chronic colitis, but this was abolished in the mice treated with anti–IL-23 mAb, accompanied by decreased expression of IFN-γ and IL-17.[37] Thus, it appears that *H hepaticus* stimulates antigen-presenting cells, such as dendritic cells and Mϕs, and the consequent production of IL-23 by these cells and the sequential induction of IFN-γ by intestinal NK cells might be involved in this model. Further studies will be needed using other types of stimuli to assess the possible role of IL-12, IL-15, or IL-18 on IFN-γ production.

Interestingly, in contrast to the effects of blocking IL-23 using neutralizing anti–IL-12/23p40 mAb, the addition of IL-23 induces only a small amount of IFN-γ production from intestinal NKp46+ NK cells (Figure 7*A* and Supplementary Figure 4). In addition, IFN-γ production by intestinal NKp46+ NK cells was greatly reduced by inhibiting their direct cell-to-cell interaction with CD14+LPMϕs using the transwell culture system (Figure 6). Because soluble TL1A was not detected in supernatant of the culture of whole LPMCs by commensal bacterial antigen stimulation,[29] membrane-bound type TL1A of CD14+LPMϕs might be associated with activation of LPNK cells.

In conclusion, we showed that the NKp44+/NKp46+ NK cell is balanced in human normal intestinal mucosa, and that this balance is disturbed in the intestinal mucosa in IBD, especially in CD. Moreover, the interaction between intestinal NKp46+ NK cells and CD14+LPMϕs is an important participant in the pathogenesis of CD via NK cell–derived IFN-γ production in response to commensal bacteria. These findings suggest that IFN-γ–producing NKp46+ mucosal NK cell subset might be involved in the pathogenesis of IBD, especially in CD.

Supplementary Material

Note: To access the supplementary material accompanying this article, visit the online version of *Gastroenterology* at www.gastrojournal.org, and at doi: 10.1053/j.gastro.2010.05.040.

References

1. Xavier RJ, Podolsky DK. Unravelling the pathogenesis of inflammatory bowel disease. Nature 2007;448:427–434.
2. Hibi T, Ogata H. Novel pathophysiological concepts of inflammatory bowel disease. J Gastroenterol 2006;41:10–16.
3. Hisamatsu T, Ogata H, Hibi T. Innate immunity in inflammatory bowel disease: state of the art. Curr Opin Gastroenterol 2008; 24:448–454.
4. Mizoguchi A, Mizoguchi E. Inflammatory bowel disease, past, present and future: lessons from animal models. J Gastroenterol 2008;43:1–17.
5. Fuss IJ, Neurath M, Boirivant M, et al. Disparate CD4+ lamina propria (LP) lymphokine secretion profiles in inflammatory bowel disease. Crohn's disease LP cells manifest increased secretion of IFN-gamma, whereas ulcerative colitis LP cells manifest increased secretion of IL-5. J Immunol 1996;157:1261–1270.
6. Matsuoka K, Inoue N, Sato T, et al. T-bet upregulation and subsequent interleukin 12 stimulation are essential for induction of Th1 mediated immunopathology in Crohn's disease. Gut 2004;53:1303–1308.
7. Sartor RB. Mechanisms of disease: pathogenesis of Crohn's disease and ulcerative colitis. Nat Clin Pract 2006;3:390–407.
8. Vivier E, Tomasello E, Baratin M, et al. Functions of natural killer cells. Nat Immunol 2008;9:503–510.
9. Jonsson AH, Yokoyama WM. Natural killer cell tolerance licensing and other mechanisms. Adv Immunol 2009;101:27–79.
10. Schepis D, Gunnarsson I, Eloranta ML, et al. Increased proportion of CD56(bright) natural killer cells in active and inactive systemic lupus erythematosus. Immunology 2008;126:140–146.